PHOSPHOPROTEOMIC ANALYSIS OF CLASS IA P110β ISOFORM-SPECIFIC SIGNAL TRANSDUCERS UPON PI3K PATHWAY ACTIVATION

A THESIS SUBMITTED TO

THE GRADUATE SCHOOL OF ENGINEERING AND SCIENCE OF BILKENT UNIVERSITY

IN PARTIAL FULFILLMENT OF THE REQUIREMENTS FOR THE DEGREE OF

MASTER OF SCIENCE

IN

MOLECULAR BIOLOGY AND GENETICS

By Beril Daloğlu

August 2023

PHOSPHOPROTEOMIC ANALYSIS OF CLASS IA P110β ISOFORM-SPECIFIC SIGNAL TRANSDUCERS UPON PI3K PATHWAY ACTIVATION

By Beril Daloğlu

August 2023

We certify that we have read this thesis and that in our opinion it is fully adequate, in scope and in quality, as a thesis for the degree of Master of Science.

Onur Çizmecioğlu (Advisor)

Bahar Değirmenci Uzun

Tunca Doğan

Approved for the Graduate School of Engineering and Science:

Orhan Arıkan

Director of the Graduate School

ABSTRACT

PHOSPHOPROTEOMIC ANALYSIS OF CLASS IA P110β ISOFORM-SPECIFIC SIGNAL TRANSDUCERS UPON PI3K PATHWAY ACTIVATION

"Beril Daloğlu"

M.S. in Molecular Biology and Genetics

Advisor: Onur Çizmecioğlu

August 2023

PI3K pathway activation is a common event observed in various human cancers. As it regulates cell proliferation, migration and metabolism, it has been widely targeted for anticancer therapies and alteration of drug resistance. Studies focusing on PI3K Class IA isoform-specific inhibition has become critical to achieve alternative targeted treatment methods. Although previous findings show that Class IA isoforms differ in their routes of activation, the downstream targets specific to the isoforms have not been fully profiled yet. This study focuses on the phosphoproteomic analysis of p110β isoform-specific downstream molecules upon PI3K pathway activation.

We have created a doxycycline-inducible system in Mouse Embryonic Fibroblasts (MEFs) to express wildtype PIK3CB gene encoding p110β or its catalytic and helical domain over-activating mutants, E1051K and N553S. By immunoblotting, the changes in downstream phosphorylation events were analyzed for MEF p110β mutants or for MEF p110β WT cells upon mitogenic PI3K stimulation. These results were collaborated with the comparative phosphoproteomic data obtained from LC-MS/MS Mass Spectrometry analysis.

Our findings show that upon short-term stimulation of the PI3K pathway, proteins associated with transcriptional regulation, cytoskeletal rearrangement, cellular signalling,

migration and metabolism are differentially phosphorylated. After longer stimulations on the other hand, proteins involved in cell cycle progression, phosphatase activity, nucleocytoplasmic transport and RNA metabolism become more prominent in the comparative phosphoproteome.

Similar to early response proteins in β WT cells, the phosphoproteome of β E1051K cells were associated with cytoskeletal rearrangement and cellular migration. Aligning with the morphological changes observed, proteins involved in anatomical structure regulation were found. Additionally, some tumour suppressors and oncogene proteins were found among the differentially regulated phosphoproteins. On the other hand, the phosphoproteome of β N553S cells were enriched for functions of RNA metabolism, nuclear import and apoptotic regulation. Proteins involved in structural organization and microtubule assembly were also observed.

37 kDa Akt substrate Poly(rC) Binding Protein 1 (Pcbp1) was found as a common differentially phosphorylated protein in the phosphoproteomes of mutant and WT p110β expressing cells. It is an RNA-binding protein associated with metastasis and EMT, and has a critical role in gene expression by coordinating RNA stability and processing. As our results have shown that p110β isoform has a major role in cytoskeletal reorganization, cell migration and transcriptional regulation, studying the regulation of p110β-Pcbp1 axis can pave the way to understand the mechanisms of increased tumour progression in p110β-dependent cells.

Keywords: PI3K pathway activation, PIK3CB, E1051K, N553S, p110β-dependence, mitogenic stimulation, mass spectrometry, phosphoproteomics, cytoskeletal reorganization, cellular migration, transcriptional regulation, Pcbp1, tumour progression, metastasis

ÖZET

PI3K SİNYAL YOLAĞI ETKİNLEŞMESİ ÜZERİNE SINIF 1A P110β IZOFORMUNUN SİNYAL İLETİCİLERİNİN FOSFOPROTEOMİK ANALİZİ

"Beril Daloğlu"

Moleküler Biyoloji ve Genetik, Yüksek Lisans

Tez Danışmanı: Onur Çizmecioğlu

Ağustos 2023

PI3K sinyal yolağı etkinleşmesi çeşitli kanserlerde yaygın görülen bir olaydır. Hücre büyümesi, göçü ve metabolizmasını düzenlemesi nedeniyle bu sinyal yolağı kanser terapisi ve ilaç direncinin kırılması üzerine yapılan çalışmalarda sıkça hedef alınmıştır. PI3K Sınıf IA izoformlarına odaklanan çalışmalar belirli molekülleri hedef alan farklı tedavi yöntemlerinin uygulanabilmesi için önemli bir hale gelmiştir. Hali hazırdaki bulgular Sınıf IA izoformlarının etkinleşme hatlarının farklı olduğunu gösterirken izoformlara özgü aşağı yöndeki hedef moleküller daha önce tümüyle tanımlanmamıştır. Bu çalışma PI3K sinyal yolağının etkinleşmesi sonrasında p110β izoformuna özgü aşağı yöndeki moleküllerin fosfoproteomik analizine odaklanmaktadır.

Bu amaçla öncelikle p110β izoformunu kodlayan PIK3CB genini ya da bu genin katalitik (E1051K) ve helikal bölge (N553S) mutantlarını fare embryonik fibroblast hücrelerinde ifade eden doksisiklin indüksiyon sistemi yarattık. Immunoblotting deneyleri ile aşağı yöndeki fosforilasyon olayları MEF p110β mutant hücreler ya da PI3K etkinleştirmesi sonucu MEF p110β yabanıl tip hücreler için analiz edilmiştir. Sonuçlarımız Sıvı Kromatografi-Kütle Spektrometresi (LC-MS/MS) ile elde edilen karşılaştırmalı fosfoproteomik veri ile desteklenmiştir.

Bulgularımızın gösterdiği üzere PI3K sinyal yolağının kısa süreli etkinleştirilmesi sonucu transkripsiyon ve hücre iskeleti düzenlemesi, hücre içi sinyal iletimi, hücre göçü ve metabolizması ile ilgili proteinler açlık durumundaki hücrelere göre ayrımsal bir şekilde fosforile edilmektedir. Bunun yanı sıra, uzun süreli uyarılma sonucu hücre döngüsünün ilerlemesi, fosfataz etkinliği, nükleositoplazmik taşıma ve RNA metabolizması ile eşleştirilen geç cevap proteinlerine karşılaştırmalı fosfoproteom içerisinde sıkça rastlanmıştır.

Yabanıl tip β hücrelerinde kısa süreli etkinleşme sonucu rastlanan proteinlere benzer şekilde β E1051K mutant hücrelerinin fosfoproteomu da hücre iskeleti düzenlemesi ve hücre göçü ile alakalı proteinler ile eşleştirilmiştir. Bu hücrelerde gözlemlenen morfolojik değişimlere paralel olarak hücre anatomisinin düzenlenmesinde görev alan proteinler de bulunmuştur. Ayrıca, bazı tümör baskılayıcı ve onkogen proteinleri de ayrımsal olarak fosforile edilen proteinler arasında yer almıştır. Öte yandan, β N553S hücrelerine ait fosfoproteomun yabanıl tip β hücrelerinde uzun sürede etkinleşme sonucu elde edilen proteinlere benzer şekilde RNA metabolizması, nükleer import ve apoptozun düzenlenmesi görevleri açısından zengin olduğu gözlemlenmiştir. Yapısal düzenleme ve mikrotübül montajında görev alan proteinlere de rastlanmıştır.

37 kDa boyutundaki Akt substratı Poly(rC) Binding Protein 1 (Pcbp1), mutantların ve yabanıl tip p110β'yı ifade eden hücrelerin fosfoproteomu arasında ayrımsal şekilde fosforile edilen ortak bir protein olarak bulunmuştur. RNA'ya bağlanma özelliği olan bu protein metastaz ve epithel-mezenkimal geçiş (EMT) ile ilişkilendirilmiştir. Ayrıca RNA kararlılığı ve işlenmesini yönetmesi nedeniyle gen ifadesi üzerinde önemli bir göreve sahiptir. Bu çalışmanın sonucunda elde ettiğimiz sonuçlara göre p110β izoformunun hücre iskeletinin ve transkripsiyonun düzenlenmesi ile hücre göçü üzerinde kayda değer bir etkisinin olması p110β-Pcbp1 ekseninin düzenlenmesinin p110β bağımlı hücrelerdeki tümör ilerlemesinin mekanizmalarını anlamamız konusunda öncü bir görev oynayabileceğini ortaya koymaktadır.

Anahtar Kelimeler: PI3K sinyal yolağı etkinleştirmesi, PIK3CB, E1051K, N553S, p110β bağımlılığı, mitojenik uyarım, kütle spektrometresi, fosfoproteomik, hücre iskeletinin düzenlenmesi, hücre göçü, transkripsiyon düzenlemesi, Pcbp1, tümör ilerlemesi, metastaz

To those who are trying to walk

their own unique path

ACKNOWLEDGEMENTS

My Master's journey has been a unique one with many challenges and so much of growth both personally and professionally. I started this journey with a wide curiosity and eagerness to learn how to think and function like a scientist on a daily basis. I have learned, unlearned and relearned everything from scratch over and over. I have faced many unfortunate and challenging situations and developed an attitude that is grounded in taking things lightly, and every experience as an opportunity to get closer to the universal knowledge, the truth and the person that I am. I believe there is not a better way than studying biology for one to carve herself into an apprentice of life and to find the courage and consistency to try again every single day.

Now that I am at the end of this chapter, getting ready to fly off to my next journey with a greater curiosity, bravery and wisdom, I must say that I have received a lot of support and love until this point. I would like to start by expressing my gratitude to Onur Çizmecioğlu, who has bestowed upon me the ability to communicate scientific knowledge in the simplest and most accurate way since my undergraduate years. He has given me the space to build my own manner of work and liberty to make mistakes and to transform them into wisdom. Although I chose to follow an unconventional path for my future studies, there hasn't been a day I did not receive his support and belief in me. I am aware that this is a very rare gift; I feel blessed and forever grateful for this.

I also want to thank Ogün Adebali and Bahar Değirmenci Uzun for all the knowledge they transplanted on me during my undergraduate years and their support as I am transitioning into the next chapter of my life.

I would like to thank our OC lab group. Once anyone enters into our lab zone, I think they know they made the right choice. You are a wonderful group of people not only with so much brains and potential but also with a sense of collaboration. I figured out countless solutions to my non-functional experiments thanks to the brainstorming we did together.

My girls, Mahnoor, Öykü and Sera… You girls came into my life when I needed you the most. You have been my guardian angels and source of daily motivation for the past three years. You brought so much joy and empathy into my life; not a single day passes without thinking of you and how lucky I am that the universe has gifted me with you.

My dear friends Ceren and Rue, you are the treasures I kept from my undergraduate years. We have learned so much together and apart. You have always been there when I needed your friendship and support. You were a source of light in my darkest times. I value both of you more than you know and I believe we have so much yet to learn together.

I must also mention my friends with whom we parted our ways. I spent nearly every night of the first two years of my Master's with you. You made me forget all the stress and pressure of the day for so long. I hope you are in a better place now.

My fiancée Oğuz, you are my day and night. We manifested and built a life of love, understanding and freedom together. You are my partner in this life and I believe life brought us together to hold each other's hands while we dare to experience our unique journeys.

Finally, I would like to send a giant wave of gratitude to my parents, my grandparents and my little sister. You are my roots and the source of my willpower. Every single day, I dare to dream of and believe in a better world because of the seeds you sowed. Thank you for raising me as a kind hearted and honest person above all else.

I also want to thank the laboratory of Prof. Pedro Cutillas at Barts Institute, Queen Mary University for collaborating with us and bringing this valuable high-throughput data into life.

I would like to thank the Newton Fund for funding our project NAF/R2/192088, and to TUBITAK for supporting me with BİDEB 2210A Scholarship.

TABLE OF CONTENTS

LIST OF FIGURES

LIST OF TABLES

ABBREVIATIONS

PI3K	Phosphatidylinositol-3 kinase
PIP3	Phosphatidylinositol-3,4,5-triphosphate
PIP2	Phosphatidylinositol-4,5-bisphosphate
AKT	Protein Kinase B
PTEN	Phosphatase and tensin homolog,
mTOR	Mammalian target of rapamycin
RTK	Receptor tyrosine kinase
GPCR	G-Protein coupled receptor
PDGF	Platelet-derived growth factor
LPA	Lysophosphatidic acid
MEF	Mouse Embryonic Fibroblast
β WT	Tet-On p110β wildtype
β EK	Tet-On p110β E1051K mutant
β NS	Tet-On p110β N553S mutant
α WT	Cumate-inducible p110α wildtype
SRB	Sulforhodamine B
PKC	Protein Kinase C
PRAS40	Proline-rich Akt substrate of 40 kDa
LC-MS	Liquid chromatography-mass spectrometry
Pcbp1	Poly(rC) Binding Protein 1 (Pcbp1)
RBP	RNA-binding protein

1. INTRODUCTION

1.1. PI3K Pathway

Phosphoinositide 3-kinase (PI3K) pathway is one the most frequently altered pathways in human cancers. As it regulates cellular proliferation, migration and metabolism, this pathway has been widely studied in cancer therapy research. It has been observed that activation of PI3K pathway induces tumorigenesis and prevents anticancer therapy responses [1]. Once activated, PI3Ks catalyse the phosphorylation of phosphoinositide on 3'OH group resulting in the conversion of phosphatidylinositol-4, 5 biphosphate (PIP_2) into phosphatidylinositol-3, 4, 5 triphosphate (PIP_3). Ser/Thr kinase Akt is then recruited to the plasma membrane and following its activation by mTOR2 and PDK1 phosphorylations, it can initiate downstream signalling cascades [1]. PIP_2 to PIP_3 conversion can be reverted by tumour suppressor *PTEN* activation.

1.2. Catalytic Subunits of PI3K

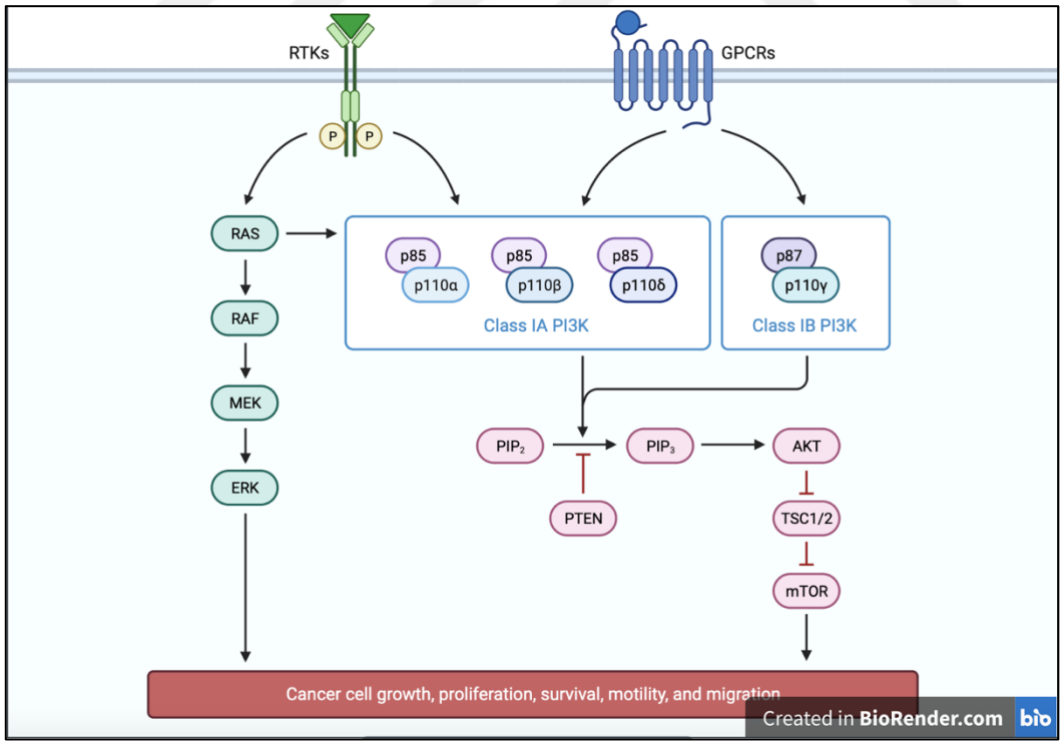

Figure 1.1: PI3K Pathway. Class IA PI3Ks can be activated through growth factor and GPCR signalling. Pathway activation results in PIP_2 to PIP_3 conversion which can be reversed by PTEN activity. *Created by BioRender* [2].

PI3Ks are membrane-bound lipid kinases comprised of three main classes: class I, II and III. Members of these classes can be made up of p110 catalytic subunits, and p85 or p55 regulatory subunits [3]. The most frequently studied class I PI3Ks are divided into two subgroups class IA and class IB. Class IAs are mainly activated by signals from receptor tyrosine kinases (RTKs), G-protein coupled receptors (GPCRs) and small G-proteins [3]. Catalytic subunits of class IAs p110α, p110β and p110 δ are encoded by *PIK3CA, PIK3CB* and *PIK3CD* genes respectively. *PIK3CA* and *PIK3CB* genes are ubiquitously expressed when *PIK3CD* expression is specific to the immune system. Therefore, there has been more extensive research on p110α and p110β subunits. p85 regulatory subunit heterodimerizes with the p110α and p110β catalytic subunits and stabilizes their kinase activity through inhibitory interactions [1]. Although both enzymatic and structural properties of these subunits are the same, recent studies have shown that they are functionally divergent.

Research with mice models has demonstrated the prevalence of p110α activity over p110β in vascular endothelial growth factor (VEGF) signaling and angiogenesis [4]. Activity of p110α can be regulated through RAS GTPase activation. Active RAS binds p110α on its N-terminal RAS-binding domain (RBD) rendering p110α into its active form. This mechanism works synergistically with tyrosine-phosphorylated proteins to optimize RTK activation through binding p85 regulatory subunit to release its autoinhibitory activity [5]. A competition model between p110α and p110β in HER2-positive breast cancer proved that p110α is more active than its isoform and enhanced tumorigenesis was observed in p110β knockouts [6]. Although relatively insensitive to growth factor stimulation through RTKs, p110β has been shown to be essential for prostate tumorigenesis [7] and pancreatic adenocarcinoma in *PTEN*-loss mice models [8]. p110β function has been observed to be significant in PI3K activation by small G-proteins and GPCRs. RHO family GTPase RAC and CDC42 bind p110β on its RBD

to activate it. Coupling of GPCRs to PI3Ks seems to be dependent on their subsequent interaction with RAC-activated p110β. Studies on p110β RBD mutant MEFs showed decreased PI3K activity and resistance to LPA-signaling related bleomycin-induced lung fibrosis [5].

1.3. Mitogenic Stimulation of Catalytic Subunits

1.3.1. Growth Factors

As serum is a mixture of various hormones, enzymes and lipids, it provides initiative signals for many different cellular processes including growth, survival and metabolism. Therefore, activation of both p110α and p110β is achieved in a cell through combinations of RTK and GPCR signaling upon serum stimulation [9].

RTKs play an essential role in PI3K/AKT signaling by transmitting external stimuli to the cellular signaling circuits. Epidermal growth factor receptor (EGFR) and platelet-derived growth factor receptor (PDGFR) are transmembrane tyrosine kinase receptors which respond to growth factor stimuli such as EGF and PDGF respectively. Overexpression of PDGFR along with its ligands has been observed in solid tumors [10]. Alterations in EGFR such as gene amplification, somatic mutations and structural rearrangements have also been implicated in human cancers [11]. Although activity of both p110α and p110β isoforms have been reported upon RTK stimulation, the role of p110α in RTK signaling has been highlighted. Growth factor signaling has been observed to be deficient in PIK3CA knockout MEFs as they resisted oncogenic transformation and failed to differentiate into adipocytes [12].

1.3.2. Insulin

By producing metabolites and hormones such as insulin, the endocrine system supplies extracellular cues which connect nutrient availability to cell proliferation, metabolism and survival. When levels of glucose in blood increase, pancreatic β-cells secrete insulin which

circulates in the bloodstream until it binds to an insulin cell surface receptor. As a result, tyrosine kinase domain of the receptor gets activated and catalyzes the phosphorylation of insulin receptor substrate proteins 1 & 2 (IRS1 & IRS2). This causes the activation of multiple signaling pathways in the cell including PI3K pathway. The insulin-PI3K pathway signaling axis is evolutionarily conserved and observed in cells of every tissue type in humans, although the responses are specific to the cell type [13].

PI3K isoform specific studies in the context of insulin signaling have shown p110α to be more prevalent than p110β. Mice with muscle-specific knockouts of p110α and p110β were created in a research study regarding skeletal muscle insulin resistance which shows decreased PI3K activation. Impaired insulin signaling and reduction in muscle size were observed only in p110α knockouts, not p110β [14]. Another research has also demonstrated that liver-specific p110α deletion results in insulin insensitivity, decreased PIP_3 production and loss of Akt activation by insulin. These defects could not be rescued by the overexpression of p110β isoform [15].

1.3.3. Lysophosphatidic Acid (LPA)

Lipid signaling with GPCRs plays a significant role in PI3K pathway activation specifically through the p110β catalytic isoform. The glycerophospholipid lysophosphatidic acid (LPA) activates various GPCRs through the Gαi/oβγ proteins, which in turn stimulates the PI3K/AKT signaling pathway. LPA can be found in nearly all types of mammalian tissues. Upon its stimulation, activated AKT enhances cell survival as it may also contribute to cell migration and proliferation. This highlights the importance of LPA on several malignancies such as cancer [16].

Recent research has shown that LPA receptors are highly abundant in cervical cancer cells and LPA provides protection against Cisplatin-mediated cell death through PI3K/AKT pathway. In the context of LPA signaling, phospho-Ser473 (pS473) AKT levels in HeLa cells were unaltered upon the inactivation of mTORC2, which is commonly associated with AKT phosphorylation on Ser473 residue. On the other hand, decrease in pS473 AKT levels was observed in MCF7 cells. This result puts an emphasis on the activation of various pathways through different LPA receptors abundant in different cell lines. This should be taken into consideration especially in anti-tumor treatments [16].

1.4. PI3K Catalytic Subunit Mutants

PI3K/AKT/mTOR pathway activation is frequently observed in tumorigenesis. Although mutations in *PIK3CA* gene encoding p110α catalytic subunit are prevalent in oncogenicity, mutations in *AKT1* – downstream effector - and, *PIK3R1* and *PIK3R2* - regulatory subunits of PI3K – are also observed to be enhancing the pathway activation. The tumor suppressor *PTEN* is also mutated or deleted in several cancers causing PI3K hyperactivation. Inhibitor treatments targeting the overactivated proteins, AKT, p110 catalytic subunits, and mTOR, have been studied clinically for disease phenotype alterations. However, drug-resistance phenotype is frequently observed over long-term exposure to the inhibitors and longevity of treatment response is precluded. Therefore, understanding the mechanism of drug resistance is crucial for effective treatment strategies [17].

Studying the differences in functional mechanisms of p110 catalytic isoforms of PI3K bears both theoretical and clinical importance as they may reveal some key feedback interactions which can be used to generate alternative treatment methods. Understanding the differential downstream events of catalytic isoforms can also explain why the cell evolutionarily

requires multiple structurally and enzymatically similar isoforms. This can bring insight into how oncogenicity of isoform-specific mutations might be altered.

1.4.1. *PIK3CA* Mutations

One of the easiest ways to study the differential effects of p110 isoforms is to observe cellular metabolic activities in mutant cell lines. *PIK3CA H1047R* and *E545K* hotspot mutations have been frequently identified in inhibitor resistant cell lines. The mechanism of resistance was found to be dependent on the reactivation of PI3K pathway together with some parallel pathways [17]. *PIK3CA H1047R* is a gain-of-function mutation on the kinase domain of PIK3CA protein [18]. Studies in mouse mammary tumor models have shown that inhibitor resistance is supported by *Myc* oncogene activation along with overexpression of ribosomal protein S6 kinase and gene amplification of the eukaryotic translation initiation factor 4E (*eIF4E*) [17]. *PIK3CA E545K* is also a gain-of-function hotspot mutation but on the PIK helical domain of PIK3CA protein [19].

Molecular Dynamics simulations investigating the conformational changes in p110α E545K mutant have shown that p85α regulatory subunit domain nSH2 PI3Kα spontaneously detaches from p110α catalytic subunit helical domain. This results in a lack of communication between the catalytic and regulatory subunits which causes pathway reactivation [20]. *PIK3CA* amplification has also been identified in breast invasive ductal carcinoma and squamous cell lung carcinoma [21] and it was associated with poor prognosis in gastric cancer [22].

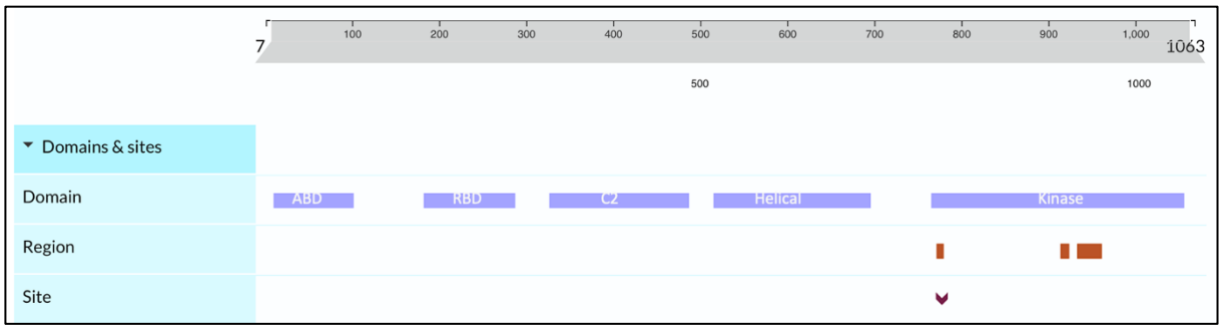

Figure 1.2: *PIK3CA* domains and sites. 1063 amino acid long *PIK3CA* is composed of an adaptor-binding domain (ABD), a Ras-binding domain (RBD), a C2 domain, a helical domain and a lipid kinase catalytic domain [23].

1.4.2. *PIK3CB* Mutations

Unlike p110α which is highly encountered as mutated in human cancers, p110β is more frequently observed to be overexpressed. Anchorage-independent growth assays with chicken embryo fibroblasts have shown that overexpression of p110β is sufficient for anchorage-independent growth which indicates tumorigenesis [24]. On the other hand, tumorigenic activity is observed for p110α only upon the overexpression of its mutant. This puts an emphasis on the oncogenic significance of p110β amplification. In PTEN-loss and p110α wildtype cell lines especially, the role of p110β seems to be critical in cell proliferation and tumorigenesis [24].

Through the analysis of frequently mutated residues in tumor samples from various cell lineages and genome-wide screening, some PIK3CB mutations have also been identified. Helical domain mutant E633K and kinase domain mutant D1067V have been observed to be driving cell proliferation, PI3K signaling and tumorigenesis [25]. In metastatic castrate resistant prostate cancer, another kinase domain mutant E1051K was identified. The functional characterization of this mutant shows that is a gain-of-function mutation which renders p110β dependence and it induces PI3K pathway activation, cell proliferation and tumorigenesis [25].

Research on PTEN-null cell lines with resistance to pan-PI3K inhibitor GDC-0941 has also revealed another PIK3CB mutant, D1067Y. This deleterious mutation (SIFT prediction) [26] seems to be at the end of p110β catalytic domain [27]. It is an activating mutant and it increases membrane-bound PIP_3 levels along with phospho-AKT and PI3K signaling. Transforming activity was also observed in nontumorigenic Rat2 cells [24].

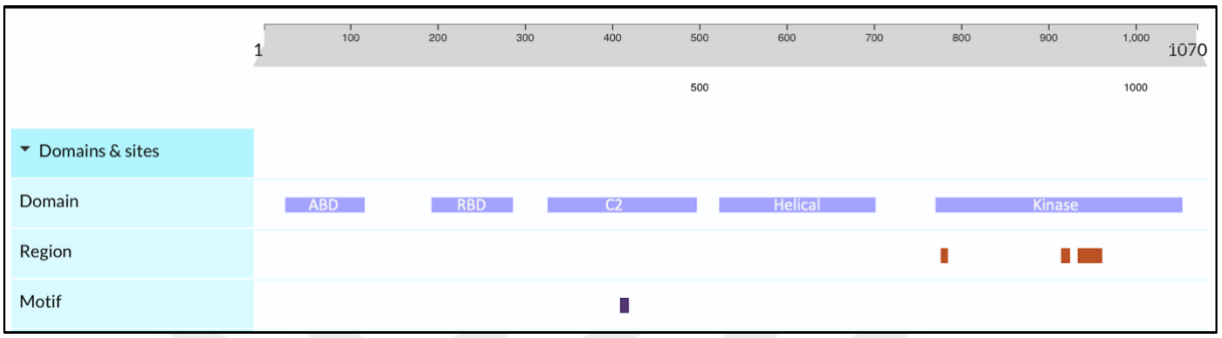

Figure 1.3: *PIK3CB* domains and sites. 1070 amino acid long *PIK3CB* is composed of an adaptor-binding domain (ABD), a Ras-binding domain (RBD), a C2 domain, a helical domain and a lipid kinase catalytic domain [27].

1.4.3. *PIK3CD* Mutations

Heterozygous gain-of-function mutations in p110δ encoding PIK3CD gene have been most commonly associated with Activated phosphoinositide 3-kinase δ syndrome (APDS), an autosomal dominant primary immunodeficiency. Mutations were identified with amino acid changes E1021K in the kinase domain, E525K and E525A in the helical domain, and N334K and C416R in the C2 domain of the leukocyte-specific p110δ subunit [28].

Research on patient samples has shown that these mutations result in PI3K hyperactivation, increased AKT phosphorylation and changes in T and B cell function. Therefore, p110δ-specific inhibitors or mTOR inhibitors like rapamycin have been suggested for treatment of patients with PIK3CD gain-of-function mutations [29].

Moreover, it should be noted that the adaptor-binding ABD domain binds p85 regulatory domain which makes inhibitory interactions with the helical, kinase and C2 domains of p110δ (Figure 1). Hence, mutations in ABD domain are expected to affect these inhibitory interactions and result in pathway hyperactivation [28].

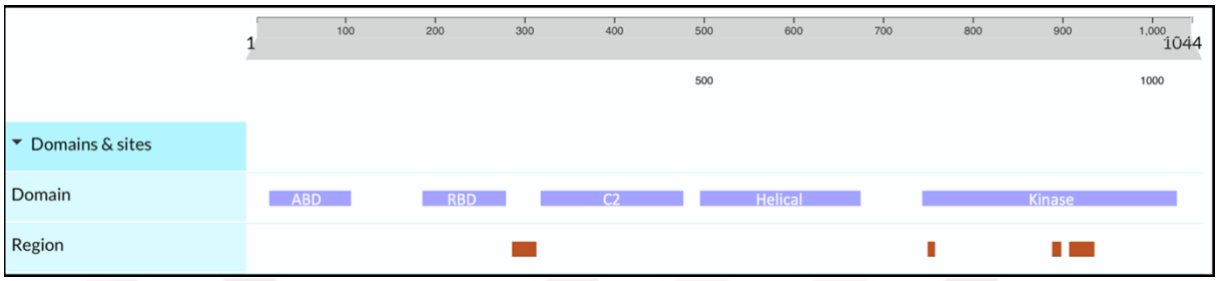

Figure 1.4.3: PIK3CD domains and sites. 1044 amino acid long PIK3CD is composed of an adaptor-binding domain (ABD), a Ras-binding domain (RBD), a C2 domain, a helical domain and a lipid kinase catalytic domain [30].

1.5. Aim of the Study

Although it is known that class IA PI3K catalytic subunits differ by their routes of activation, it is not clear how these differences affect the downstream signaling and cellular events such as proliferation and metabolism. By using serum and various mitogens such as PDGF, insulin and LPA to stimulate the catalytic subunits, downstream protein signaling is aimed to be altered in an isoform-specific manner. Through the quantitative and qualitative analyses of these downstream proteins and their phosphorylated forms, it is aimed to identify isoform-specific functions of p110β and related protein networks which can be studied further to bring forth a novel perspective into cancer therapy research. Furthermore, studying p110β specific mutants may propose connections between mitogenic stimulation and tumorigenic alterations in signalling components and cellular activities. This study focuses on the high-throughput phosphoproteomic analysis of p110β-dependence in a dox-inducible p110β WT

molecular genetic system along with the kinase and helical domain mutants, E1051K and N553S.

2. MATERIALS & METHODS

2.1. Materials

2.1.1. Cell Lines & Growth Media

Table 2.1: Cell lines and their corresponding complete growth media recipe for maintenance.

Cell Line	Growth Medium
MEF or MEF rtta	DMEM High Glucose, 8% FBS, 1% P/S, 1% NEAA
MEF β WT (Tet-On p110β wildtype) MEF β EK (Tet-On p110β E1051K mutant) MEF β NS (Tet-On p110β N553S mutant)	DMEM High Glucose, 8% Tet-Free FBS, 1% P/S, 1% NEAA
MEF α WT (Cumate-inducible p110α wildtype)	DMEM High Glucose, 8% Tet-Free FBS, 1% P/S, 1% NEAA
HEK 293	DMEM High Glucose, 8% FBS, 1% P/S, 1% NEAA

2.1.2. Cell Culture Reagents

Table 2.2: Cell culture reagents used for maintenance of cell lines and cell culture-related experiments.

Catalog Number	Product Name	Brand
D6429-500mL	DMEM – Dulbecco's Modified Eagle's Medium - High Glucose	Sigma-Aldrich, US
S1810-500	Fetal Bovine Serum (FBS)	Biowest, US
FBS-TET-12A	Tetracycline-Free FBS	Capricorn, US
25300-054	Trypsin-EDTA (0.05%)	Gibco, US
15140-122	Penicillin-Streptomycin (P/S)	Gibco, US
M7145-100mL	MEM Non-Essential Amino Acid solution (100x)	Sigma-Aldrich, US
PBS10X-500	Phosphate-Buffered Saline (PBS) (10X), ph:7.4	ECOTECH, TR
L3000-008	Lipofectamine 3000	Thermo Scientific, US
631455	Retro-X Concentrator	Takara Bio, US
Sc-134220	Polybrene	Santa-Cruz Biotech, US
631449	Cre Recombinase Gesicles	Takara Bio, US
D9891-1G	Doxycyclin Hyclate	Sigma-Aldrich, US
268402-5G	4-isopropylbenzoic acid (Cumic acid/Cumate)	Sigma-Aldrich, US
AB-101L	Nourseothricin (NAT)	Jena Bioscience, Germany
10131-035	Geneticin (G418 Sulfate)	Gibco, US
A111138-03	Puromycin	Gibco, US
16986	BYL719_10mg	Cayman, US
S1462	KIN193	Shelleck Chem

S1078	MK2206	Shelleck Chem
S1120	Everolimus (RAD001)	Shelleck Chem
17258	EHT1864	Cayman, US

2.1.3. Buffers & Solutions

Table 2.3: Recipes of buffers and solutions used during experimental procedures.

Solution	Recipe
RIPA Lysis Buffer (1X)	1X RIPA 1X Protease Inhibitor 1X Phosphatase Inhibitor Mix 1 μM DTT 1 mM Sodium orthovanadate
Urea Lysis Buffer (8M)	8 M Urea in 20 mM HEPES (pH 8.0) 100 mM Sodium orthovanadate 500 mM Sodium fluoride 1 M β-glycerol phosphate 250 mM Disodium pyrophosphate
Wash Buffer with Inhibitors for Urea Lysis	1X PBS, ice-cold 500 mM Sodium fluoride 100 mM Sodium orthovanadate

NP-40 Lysis Buffer	50 mM Tris-HCl pH 7.5 150 mM NaCl 0.5% w/v NP-40 5 mM EDTA 1 mM DTT 0.1 mM Sodium orthovanadate 1X Protease Inhibitor 1X Phosphatase Inhibitor Mix
50X TAE	242 g Trizma-Base 57.1 mL Acetic Acid 100 mL EDTA (0.5M) Complete up to 1 L with ddH_2O
10X TBS	30 g Trizma-Base 80 g NaCl 2 g KCl Adjust pH to 7.4 with HCl Complete up to 1 L with ddH_2O
TBS-T	1 L TBS (1X) 1 mL Tween-20

Resolving Gel Buffer (pH 8.8)	187 g Trizma-Base Adjust pH to 8.8 with HCl Complete up to 1 L with ddH_2O
Stacking Gel Buffer (pH 6.8)	60.5 g Trizma-Base Adjust pH to 6.8 with HCl Complete up to 1 L with ddH_2O
10X Running Buffer for Western Blot	144 g Glycine 30 g Trizma-Base 10 g SDS Complete up to 1 L with ddH_2O
10X Transfer Buffer for Western Blot	144.1 g Glycine 30.3 g Trizma-Base Complete up to 1 L with ddH_2O
1X Transfer Buffer for Western Blot	100 mL Transfer Buffer (10X) 200 mL Methanol 700 mL ddH_2O

5% Blocking Solution	5 mg BSA Fraction V or milk powder 100 ml TBS-T (1X)
Sulforhodamine B Dye Solution (SRB)	0.4% SRB (w/v) in Acetic Acid (1%)
Trichloroacetic Acid (TCA)	50% TCA (w/v) in ddH_2O
Cell Fixation Solution	4% Paraformaldehyde (PFA) in PBS (1X)
Destaining Solution	10 mM Trizma-Base in ddH_2O (pH 10.0)

2.1.4. Western Blot Reagents

Table 2.4: List of reagents used during Western Blot and related sample preparation.

Catalog Number	Product Name	Brand
10688.01	Acrylamide/Bisacrylamide (30w/v)	Serva, Germany
161-0747	4x Laemlie Buffer	Bio-Rad, USA
A40000279	Pierce™ Coomassie Plus (Bradford) Assay Reagent	Thermo Scientific, USA
11930.03	Albumin Bovine Fraction V pH 7.0	Serva, Germany
K-12045-D20	WesternBright ECL Kit	Advansta, USA
773301	Prime-Step Protein Ladder	BioLegend, USA
23391.02	Glycine	Serva, Germany

P0758S	Sodium Orthovanadate	New England Biolabs, USA
39055.01	Phosphatase Inhibitor Mix	Serva, Germany
PIC002.1	Protease Inhibitor Cocktail, Powder without EDTA	BioShop, Canada
GE10600003	Nitrocellulose Blotting Membrane	Merck, Germany
PS05	ClearBand Ponceau S	EcoTech, Turkey
2502	ReBlot Plus Mild Stripping Solution, 10X	Merck, Germany
2504	ReBlot Plus Strong Stripping Solution, 10X	Merck, Germany
10426890	Whatman Gel Blot Paper	GE Healthcare Life Sciences, USA
M3148-250ML	2-Betamercaptoethanol	Sigma-Aldrich, USA
8.22050.100	SDS	Millipore, Germany
39796.51	Tween 20	Serva, Germany
1.107.320.100	TEMED	Millipore, Germany
24137-2.5L-R	Isopropanol	Sigma-Aldrich, USA
24229-2.5L-R	Methanol	Sigma-Aldrich, USA

2.1.5. Antibodies

Table 2.5: List of antibodies used during Western Blot or immunocytochemistry.

Catalog Number	Product Name	Brand

R-05071-500	Anti-Mouse IgG, HRP-linked	Advansta, USA
7074S	Anti-Rabbit IgG, HRP-linked	Cell Signaling Technology, USA
3873S	α-Tubulin (DM1A) Mouse mAb	Cell Signaling Technology, USA
2118S	GAPDH (14C10) Rabbit mAb	Cell Signaling Technology, USA
3011S	PI3 Kinase p110β (C33D4) Rabbit mAb	Cell Signaling Technology, USA
4249S	PI3 Kinase p110α (C73F8) Rabbit mAb	Cell Signaling Technology, USA
sc-376641	Anti-PI3-kinase p110β Antibody (C-8)	Santa Cruz Biotechnology, USA
680302	Purified anti-Akt1(Clone:O94E10)	BioLegend, USA
691802	Purified anti-RPS6 (Clone:A16009C)	BioLegend, USA
sc-2027	Normal Rabbit IgG	Santa Cruz Biotechnology, USA
405326	Alexa Fluor 594 Goat anti-mouse IgG (minimal x-reactivity)	BioLegend, USA
9614S	Phospho-Akt Substrate (RXXS*/T*) (110B7E) Rabbit mAb	Cell Signaling Technology, USA
4056S	Phospho-Akt (Thr308) (244F9) Rabbit mAb	Cell Signaling Technology, USA
9018P	Phospho-Akt1 (Ser473) (D7F10) XP Rabbit mAb	Cell Signaling Technology, USA
9381S	Phospho-Threonine/Tyrosine Antibody	Cell Signaling Technology, USA
2261S	Phospho-(Ser) PKC Substrate Antibody	Cell Signaling Technology, USA
2215S	Phospho-S6 Ribosomal Protein (Ser240/244) Antibody	Cell Signaling Technology, USA

4858S	Phospho-S6 Ribosomal Protein (Ser235/236) (D75.2.2E) XP Rabbit mAb	Cell Signaling Technology, USA
2691	PRAS40 (D23C7) XP Rabbit mAb	Cell Signaling Technology, USA
96215	Phospho-Tyrosine	Cell Signaling Technology, USA
ab9332	Phospho-Serine	Abcam, UK

2.1.6. Cloning Reagents

Table 2.6: List of reagents used for molecular cloning experiments.

Catalog Number	Product Name	Brand
M0202S	T4 DNA Ligase	New England Biolabs, USA
R3101S	EcoRI-High Fidelity (HF) Restriction Enzyme	New England Biolabs, USA
R3189S	NotI-High Fidelity (HF) Restriction Enzyme	New England Biolabs, USA
R3136S	BamHI-High Fidelity Restriction Enzyme	New England Biolabs, USA
M0530S	Phusion High Fidelity (HF) DNA Polymerase	New England Biolabs, USA
39793.03	Water DEPC (0.1%) treated	Serva, Germany
N3232S	1 kB DNA Ladder	New England Biolabs, USA
10835269001	Ampicillin	Roche Life Sciences, USA
C3040I	NEB Stable Competent E. coli	New England Biolabs, USA

B9035S	NEB 10-Beta/Stable Outgrowth Medium	New England Biolabs, USA

2.1.7. Cloning Vectors

Table 2.7: List of vectors used for molecular cloning experiments.

Catalog Number	Product Name	Brand
47916	pRXTN retroviral vector	Addgene, USA
	pBABE-puro PIK3CB E1051K	Homemade
	pBABE-puro PIK3CB N553S	Homemade

2.1.8. Primers

Table 2.8: List of primers designed for PCR reaction setup for molecular cloning experiments.

Primer	Sequence
β Forward NotI	5'GCCGGAT…CCATGGG3'
β Reverse EcoRI	5'CATTCCA…GGTCGAC3'

2.1.9. Kits

Table 2.9: List of various kits used during experiments.

Catalog Number	Product Name	Brand

D6492-01	E.Z.N.A Cycle Pure Kit	Omega Bio-tek, USA
K0502	GeneJET Plasmid Mini Prep Kit	Thermo Scientific, USA
169014875	Plasmid Midi Kit	Qiagen, Germany
28704	QIAquick Gel Extraction Kit	Qiagen, Germany
21071	SMART BCA Protein Assay Kit	Intron Biotechnology, South Korea

2.1.10. Equipment

Table 2.10: List of frequently used equipment.

Mini-Protean Tetra Cell	Bio-Rad, USA
Amersham Imager 600	GE Healthcare, USA
Cell Culture Hood	Nuaire, USA
CO_2 Incubator	Thermo Scientific, USA
Nanodrop One	Thermo Scientific, USA
Synergy HT Microplate Reader	Biotek, USA
Thermocycler for PCR	Bio-Rad, USA
Centrifuges	Hettich, Germany Nuve, Turkey
Fluorescence Microscope	EVOS, USA
Agarose Gel Electrophoresis System	Consort, Belgium

2.2. Methods

2.2.1. Cell Maintenance and Passaging

Cells were maintained in 10 ml growth media on 10-cm sterile cell culture dishes. They were passaged at around 80% confluency. For passaging they were washed with 2 ml 1X sterile PBS and trypsinized with 1 ml 0.05% trypsin and incubated at 37°C for 5 mins. After surface attachment was lost, trypsin activity was halted with FBS containing media and cells were centrifuged at 1500 rpm, RT for 5 mins. The supernatant was aspirated and the cell pellet was suspended in growth media (see Table 2). The cell suspension was diluted according to the desired splitting ratio and the cells were seeded onto 10 cm plates in total of 10 ml growth media. Cells with exogenous constructs were provided with selection antibiotics once in two passages. Cre-treated cells with endogenous deletions were cultivated with doxycycline or cumate (half of induction dosage) to provide growth advantage (see Table 3).

Table 2.11: Selection markers with their maintenance dosages.

Cell Line	Selection Marker	Dosage
MEF β WT Cre(+) (pRXTN rtTA PIK3CB WT)	NAT	50 ug/ml
	G418	50 ug/ml
	DOX	0.5 ug/ml
MEF β EK Cre(+) (pRXTN rtTA PIK3CB E1051K)	NAT	50 ug/ml
	G418	50 ug/ml
	DOX	0.35 ug/ml

MEF β NS Cre(+) (pRXTN rtTA PIK3CB N553S)	NAT	50 ug/ml
	G418	50 ug/ml
	DOX	0.35 ug/ml
MEF α WT (Cumate-inducible p110α wildtype expression)	G418	50 ug/ml
	Cumate	15 ug/ml
MEF rtta	G418	50 g/ml

2.2.2. Cell Thawing

Cells were taken out of liquid nitrogen and thawed in 37°C waterbath without contacting the lid of the cryovial with water. After the cells were thawed with only a small fraction of frost left, cell suspension was taken with a micropipette and diluted in 5 ml growth medium in a falcon. The suspension was centrifuged for 5 mins at 1500 rpm, RT. The supernatant was aspirated and the pellet was dissolved at 10 ml thawing medium (growth medium without P/S). After the cells were recovered with their corresponding morphologies, thawing medium was replaced with growth medium and selection antibiotics were given.

2.2.3. Cell Freezing

When the cells were in exponential growth phase (below 80% confluency) they were washed with PBS and trypsinized according to the passaging procedure. After the centrifuge, the pellet was suspended in freezing medium (40% FBS, 10% DMSO, 50% DMEM). The volume of the total freezing medium was arranged according to the number of cryovials used. For cells at ~70% confluency 3 vials were used with 1 ml cell suspension for each. After the

cells were divided into cryovials, vials were quickly transferred to Mr. Frosty and incubated at -80°C overnight. Then, vials were transferred to liquid nitrogen.

2.2.4. Starvation and Stimulation

Cells were seeded as on the day of the experiment the confluency was 70-80%. After media was aspirated, cells were washed with PBS gently. 5 ml empty DMEM was added on the plate and the cells were starved for 4 to 12 hours. If inhibition was planned, the desired concentration of the inhibitor was given onto empty DMEM half an hour before starvation was completed.

At the end of inhibition, cells were stimulated with the stimulant for either 5 or 30 minutes. To allow the stimulant to spread onto the whole plate, plate was swirled multiple times. After stimulation was completed, media was aspirated immediately and cells were given cold PBS to halt the stimulation.

Table 2.12: Inhibitors and their working concentrations.

Inhibitor	Concentration
KIN-193	2 μM
BYL-719	2 μM

Table 2.13: Stimulants and their working concentrations.

Stimulant	Concentration
PDGF	20 ng/mL
Insulin	2 μg/mL
LPA	20 μM
Serum	5%

2.2.5. Construction of pRXTN-PIK3CB-E1051K and N553S Plasmids

2.2.5.a. Polymerase Chain Reactions

Polymerase Chain Reactions (PCR) were set to anneal EcoRI and NotI sites to HA PIK3CB mutant inserts in pBabe puro vector. 30 cycles were performed with Phusion High Fidelity DNA polymerase. See Table 2.8 for primer sequences and Table 2.12 for PCR reaction conditions.

Table 2.14: PCR reaction conditions

Step	Temperature	Duration
Initial Denaturation	98°C	30 s
Denaturation	98°C	10 s
Annealing	50°C	30 s
Extension	72°C	66 s
Final Extension	72°C	7 min

2.2.5.b. Agarose Gel Electrophoresis

The agarose percentage was determined according to the molecular weights and distances expected between DNA products. For 1% gel, 1 g agarose was added to 100 mL 1X TAE Buffer. To dissolve the agarose, the mixture was microwaved for 2 minutes at high power, then it was cooled down at room temperature. 5 µl Ethidium Bromide was added and the flask was swirled until it was dissolved. The gel mixture was poured into a gel casting tray and the appropriate comb was placed on top. After the gel was solidified, the comb was taken out and the gel on the tray was placed into the tank. Tank was filled with 1X TAE buffer. Desired

amount of DNA was mixed with loading dye and loaded into the wells along with a ladder. The gel was run at 80-150 V.

2.2.5.c. Gel Extraction

3 kb PCR products were visualized with gel electrophoresis under low UV light to avoid mutations and they were excised out of the agarose gel with a razor blade. The excised gel pieces with the DNA products of interest were kept in an Eppendorf tube at -20°C. DNA products were extracted from the agarose gel according to Qiagen Gel Extraction protocol (See Catalog Number in Table 2.9. Concentrations of isolated DNA products were measured with NanoDrop.

2.2.5.d. Restriction Enzyme Digestion

The isolated PIK3CB mutant inserts and pRXTN vector were restriction enzyme digested with EcoRI & NotI HF enzymes. See Table 2.13 for reaction conditions. The reaction tube was incubated at 37°C for 30 mins and heat inactivated at 65°C for 20 mins.

Table 2.15: Restriction enzyme digestion reaction conditions.

DNA	1 μg
10X CutSmart Buffer	5 μL
NotI-HF	1.0 μL
EcoRI-HF	1.0 μL
DEPC water	Up to 50 μL

The restriction digested products were purified with E.Z.N.A Cycle Pure Kit and the concentration of purified DNA products were measured with NanoDrop.

2.2.5.e. Ligation

Required insert DNA mass was calculated with NEBioCalculator. Reaction was set according to T4 DNA Ligase protocol. See Table 2.14 for reaction conditions. Negative control reactions were set without the insert.

Table 2.16: T4 DNA Ligase reaction conditions.

pRXTN vector	121.5 ng
PIK3CB *E1051K or N553S* insert	190.7 ng
10X Ligase Buffer	2 µL
T4 DNA Ligase	8 µL (4 Weiss U)
DEPC water	Up to 20 µL

2.2.5.f. Bacterial Transformation

NEB Stable Competent E. Coli (C3040I) cells were used for transformation. 50 µl competent cell aliquots were thawed on ice and 10 µl ligation and control products were added into the cells without pipetting. The tubes were incubated on ice for 30 mins. For heat shock, cells were put into 42°C waterbath for 45 secs and then immediately put on ice for 5 min incubation. Later on, 950 µl NEB Outgrowth Medium was added onto the cells and they were incubated at 37°C in a shaking incubator for an hour. At the end of inoculation, the tubes were centrifuged at 3500 rpm for 5 mins. 900 µl of the supernatants were discarded and the pellets were dissolved in the remaining supernatants very gently. The suspensions were spread onto ampicillin containing LB-Agar plates and incubated overnight at 37°C. At the end of incubation, single colonies were picked for plasmid isolation with Thermo Scientific Mini Prep Kit or QIAGEN Plasmid Midi Kit. A starter culture was set in 3 mL LB with ampicillin in a round bottom tube. The culture was inoculated for 8 hours (logarithmic phase) at 37°C in a

shaking incubator. Then, the starter culture was diluted 1/500 into a flask with at least four times greater than the medium volume and it was inoculated overnight.

2.2.5.g. Screening

Double digestion with EcoRI and BamHI HF enzymes was applied on the ligation product to proceed to screening with gel electrophoresis.

Table 2.17: Restriction enzyme digestion reaction conditions for screening.

DNA	500 µg
10X CutSmart Buffer	2.5 µL
NotI-HF	0.5 µL
EcoRI-HF	0.5 µL
DEPC water	Up to 25 µL

2.2.6. Production of Stable Cell Lines

2.2.6.a. Lipofectamine Transfection

Viral particles were formed using Lipofectamine 3000 reagent protocol. The day before transfection, $2x10^5$ HEK293 cells were seeded onto 6-well plates. On the day of transfection, cell confluency must be 70-80%. Two separate solutions with empty DMEM were prepared for Lipofectamine 3000 and DNA. In Tube A, 3.75 µl Lipofectamine 3000 was added on 125 µl DMEM. In Tube B, 2.5 µg DNA and 5 µl P3000 were added on 125 µl DMEM. 2:1:1 ratio must be applied to total DNA amount (2.5 µg) in Tube B as following; vector:gag/pol:vsv.g. After tubes were pipetted, they were mixed together and incubated at RT for 10-15 mins. At the end of incubation, ~250 µl mixture was added to each well of HEK293 cells. The next day,

media was aspirated and fresh growth media was added. A day later, the supernatant on the wells was collected into a falcon wrapped with aluminum foil and was stored at 4°C up to a week. Before proceeding to the transduction, viral supernatant was filtered with 0.45 micron filter to get rid of any remaining cell material.

2.2.6.b. Retroviral Transduction

On the day of transduction the cell confluency must be 20% to maximize transduction efficiency; MEF rtta cells were seeded accordingly. Before transduction, 1 volume of Lenti-X concentrator was added to 3 volumes of filtered viral suspension and it was mixed with gentle inversion. The mixture was incubated 30 mins to overnight at 4°C. At the end of incubation, the mixture was centrifuged at 1500g, 4°C for 45 mins. Without moving the white pellet, the supernatant was discarded and the pellet was resuspended in the minimum volume of total media required for transduction. On the day of transduction, concentrated viral suspension was given to the transduction wells when complete growth media was given to control wells. 10 µg/mL polybrene was also added to each well. The next day, media was replenished and cells were passaged if they have reached confluency. A day later, the appropriate amount (250 ug/mL) of selection antibiotic (NAT) was given to each well. On the following days cells were observed until all cells on control wells die. After selection was completed, the maintenance dose (50 µg/mL) of NAT has been administrated regularly to the transduced cells.

2.2.7. Endogenous Gene Deletions

The endogenous PIK3CA and PIK3CB genes have been floxed prior to this study. For the protocol of the generation of $p110\alpha^{flox/flox}$; $p110\beta^{flox/flox}$ MEFs from embryos, see [31]

2.2.7.a. Adenovirus-Mediated (Ad/Cre) Cre Deletions

Cells must be seeded one day before the experiment so that the confluency will be 20-25% for maximum transduction efficiency. MEF β EK & NS cells were seeded on a 6-well plate with a density of 20,000 cells/well. Next day, growth media was aspirated and 1 mL 2% FBS media with 2 µL Ad/Cre was given to each well. 6 hours post-transduction, Ad/Cre media was discarded and complete growth media was given.

2.2.7.b. Gesicle-Mediated Cre Deletions

Cells must be plated one day before the experiment so that the confluency will be 60-80% on the day of the experiment. Cultures with confluency of less than 50% may lose viability upon treatment. MEF β EK & NS cells were seeded on a 12-well plate with a density of 37,000 cells/well. Next day, Polybrene (PB) media was prepared by adding 6 µg/mL Polybrene to the complete growth medium without Pen/Strep. Cell media were replaced by 1 mL PB media. Cre Recombinase Gesicles were thawed on ice. 10 µL of Gesicles were given to each well. Cells were incubated at 37ºC in an incubator overnight. At the end of incubation, PB media was replaced with complete growth media after passaging cells with 1:5 dilution to acquire 60-80% confluency for Round 2 next day. 3 rounds were performed in total. Deletions were verified by comparing p110β protein levels with Western Blotting.

2.2.8. Cell Harvesting

When the cells reached desired confluency, they were washed with sterile 1X PBS to get rid of residual media. Then, 5 ml ice-cold 1X PBS were given to each plate. Plates were taken out of the hood and scraped with a cell scraper. The cell suspension was collected into a falcon and centrifuged at 1500 rpm, 4°C for 8 mins. After the supernatant was discarded, the pellet was snap-frozen in the falcon and kept at -80°C.

2.2.9. Cell Lysis

2.2.9.a. RIPA Lysis for Western Blotting

RIPA lysis buffered was prepared according to the recipe on **Table 2.3**. The volume of the lysis buffered was arranged according to 1:1 ratio (pellet:buffer). After the frost on falcons started to melt, the pellet was pipetted in lysis buffer vigorously and it was incubated on ice for 30 mins. The suspension was flicked every 10 mins to promote complete lysis. At the end of incubation, suspension was transferred into an Eppendorf tube and centrifuged for 15 mins at 13000 rpm, 4°C. The supernatant was transferred into a fresh Eppendorf, snap-frozen in liquid nitrogen and stored at -80°C.

2.2.9.b. Urea Lysis for Mass Spectrometry

This procedure starts with cell harvest in urea buffer, regular harvesting procedure should not be applied.

Two plates from each experimental condition were prepared to provide sufficient amount of lysate for mass spectrometry. Cells were washed with 1 ml ice-cold PBS (1X) with inhibitors (**Table 2.3**) 3 times. After all PBS was removed, 400 µl urea lysis (**Table 2.3**) buffer was added onto each plate. Cells were scraped, collected into low-binding Eppendorf tubes and kept on ice at all times. The cell suspensions were sonicated with a probe sonicator at 40% amplitude for 15 s and rested for 25 s. This was repeated 3 more times. During sonication on/off cycles the Eppendorf tubes must remain on ice to avoid heating up the samples. After centrifuge at 14000 rpm, 4°C for 20 mins, the supernatants were transferred into fresh ice-cold low-binding Eppendorf tubes. Samples were snap-frozen in liquid nitrogen and kept at -80°C.

2.2.9.c. NP-40 Lysis for Immunoprecipitation

NP-40 lysis buffered was prepared according to the recipe on (**Table 2.3**). The volume of the buffer was arranged according to 1:2 ratio (pellet:buffer). The remaining procedure is the same as RIPA lysis.

2.2.10. Bradford Assay for Protein Quantification

Protein lysates were diluted 1:10 with ddH_2O to avoid interference of lysis reagent with Bradford reagent. Standards were prepared by diluting 2 mg/mL BSA solution according to **Table 2.16**. 5 µl of each diluted lysate and standard were added to each well of a 96-well plate. 3 replicates were prepared for each group. 250 µl Coomassie Blue Dye were added to each well and mixed on a shaker for 30 secs. After incubation at RT for 10 mins, absorbance at 595 nm was measured with a spectrophotometer. The plate must be covered with aluminum foil to avoid light after the addition of light-sensitive Coomassie Blue Dye. The protein concentrations were calculated according to the standard curve equation derived from absorbance values.

Table 2.18: Required volumes of BSA (2 mg/mL) for standard preparation.

Standard	Protein Amount (ug)	BSA (2mg/ml) Volume (µL)	ddH_2O Volume (µL)
A	10	300	0
B	7.5	375	125
C	5	325	325
D	3.75	175 from B	175
E	2.5	325 from C	325
F	1.25	325 from E	325
G	0.625	325 from F	325
H	0.125	100 from G	400

I	0	0	400

2.2.11. Western Blotting

Protein samples were prepared according to their calculated concentrations. 20-25 µg protein was generally prepared for a well. 1x Laemlie Buffer and 10% β-mercaptoethanol were used for sample preparation. For SDS-PAGE, 10% resolving and 4% stacking polyacrylamide gels were cast according to the recipe on **Table 2.17**.

Table 2.19: Ingredients and their required amount to cast one gel.

Ingredient	10% Resolving Gel	4% Stacking Gel
Acrylamide/bisacrylamide (30% w/v)	3.3 mL	0.66 mL
Resolving Gel Buffer (pH=8.8)	2.5 mL	-
Stacking Gel Buffer (pH=6.8)	-	1.26 mL
10% APS	50 µL	25 µL
TEMED	5 µL	5 µL
ddH_2O	4.1 mL	3 mL

Resolving gel was prepared first and stacking gel was poured on top of resolving. APS and TEMED were added the last to each gel solution and right before casting to avoid polymerization. 1.5 mm separating glasses, Mini Protean Gel Casting System and 10- or 15-well comb were used. After the gels were solidified, the ladder and the proteins were loaded to the wells and gels were run at constant 100 V for 90 mins. Then, proteins were transferred to nitrocellulose membranes by wet transfer at constant 250 mA for 150 mins. This was performed

on ice to avoid heating of the transfer buffer. At the end of transfer, membranes were stained with Ponceau S stain to validate transfer efficiency and after getting rid of the excess stain by washing with water, membranes were cut with a razor blade according to the molecular weights of the proteins to be visualized. Membranes were blocked with 5% BSA on a shaker for an hour at RT. Then, they were incubated with corresponding primary antibodies overnight on a shaker at 4ºC. Primary antibodies were prepared in 3% BSA with their suggested concentrations on product sheet. Next day, membranes were washed three times for 5 mins with TBS-T at RT and then incubated with HRP conjugated mouse or rabbit secondary antibodies for an hour on a shaker at RT. Secondary antibodies were generally prepared with 1:5000 – 1:10000 dilutions in 3% BSA. At the end of the incubation, membranes were again washed two times with TBS-T for 5 mins and one time with dH_2O at RT. After incubation with ECL solution for ~ 2 mins at dark, excess ECL was discarded and proteins were visualized with Amersham Imager 600.

2.2.12. Co-Immunoprecipitation

All centrifugations in this protocol were done at 3000 rpm, 4ºC for 5 mins with a microcentrifuge. After cell lysis with NP-40 (see **2.2.8.c**) and protein quantification, total required amount of protein was diluted to 1 µg/µL with NP-40 lysis buffer. 500 ug of protein lysate was incubated with the suitable antibody concentration overnight at 4ºC in an icebox. Next day, A/G Agarose beads were equilibrated by adding 50 µL beads to 500 µL lysis buffer. While pipetting the beads, the tip of the micropipette was cut to avoid harming the beads. The beads were centrifuged and the lysis buffer was discarded. The bead pellet was resuspended in 50 µL lysis buffer by gentle flicking. Then, antibody conjugated lysate was added on top of the equilibrated beads and incubated on a rotating wheel for 30 mins at 4ºC. The mixture was centrifuged and the supernatant was discarded. Antibody-protein-bead conjugate was washed three times with 200 µL lysis buffer by gentle flicking and centrifuging. The supernatant was

discarded each time. For elution, 30 µL of Laemlie solution containing 10% β-mercaptoethanol was added on the bead conjugate. The mixture was put on a heat block at 95ºC for 10-15 mins and then it was centrifuged at RT. The supernatant was collected without disturbing the bead pellet. The beads were discarded and the elute was stored at -20ºC. Western Blotting was performed with co-immunoprecipitated protein elute to check for interactions with proteins of interest.

2.2.13. Sulforhodamine B (SRB) Proliferation Assay

MEF β wt, β EK and β NS cells were seeded on 96-well plates at a density of $0.1x10^4$/well. Next day (day 0), the treatment groups were supplied with their corresponding inhibitor and serum-depleted media. At the end of treatments, plates were taken out of cell culture and the media was discarded. The cells were fixed with 50 µL 10% TCA for an hour at 4ºC. After cells were washed with dH_2O five times, they were stained with 50 µL 0.4% SRB solution for 30 mins at RT. Since SRB is light-sensitive the procedure was proceeded at dark. The cells were washed with 1% acetic acid five times and they were air-dried at RT. Then the cells were de-stained with 200 µL 10 mM Tris-base solution by pipetting. The optical density at 564 nm was measured with a spectrophotometer.

2.2.14. Mass Spectrometry

This protocol was retrieved from the laboratory of Prof. Pedro Cutillas at Barts Institute, Queen Mary University [32]. Three biological samples for each condition were prepared with urea lysis method described in **2.2.8.b**. After preparation, samples were sent to Barts Institute for Mass Spectrometry-Based Phosphoproteomics analysis. At first, alkylation and reduction of cysteines was managed at RT, in a dark room for 15 min. Then, phosphopeptides were enriched with TiO_2. Glycolic acid buffer 2, 99/1 H_2O/ACN was used to wash the packed tips

sequentially. For elution, four sequential washes with 5% NH_4OH in 1% ACN were performed. After resuspension of phosphopeptide pellets in 20 µL of 0.1% TFA and 4 µL of the suspension was loaded into an LC-MS/MS system. This system is comprised of a nanoflow ultrahigh pressure liquid chromatography (UPLC, nanoAccuity, Water) coupled online to an Orbitrap XL mass spectrometer (Thermo Fisher Scientific). In a multistage activation mode, the top five most intense multiply charged ions were chosen for collision-induced dissociation fragmentation. MS1 was configured with a 60,000 resolution.

By using the Mascot search engine, MS/MS data was searched for peptide identification from the SwissProt database restricted to mouse entries. The setting for the parent and fragment ions were set as 10 parts per million (ppm) and 600 millimass units respectively. The modifications selected were phosphorylation on Serine, Threonine and Tyrosine; oxidation of methionine and PyroGlu on N-terminal glutamine. In a database of sites that can be quantified by MS, phosphopeptides with a Mascot score less than 0.05 (~2% false discovery rate) were included. The peak heights of extracted ion chromatograms of phosphorylated peptides for all the samples under comparison were obtained using Pescal software. Pescal matched retention times along chromatograms using peptides that were present in all samples as reference points. The windows for the extracted ion chromatogram (XIC) were 6 ppm and 2 min. The max_delta score was used to express the accuracy of identified phosphorylation sites.

MSstats v3.3.1 was used to statistically analyse the quantified phosphopeptides. Each condition was replicated three times technically. To test for differing levels of abundance between conditions or screens, the group comparison tool was used. Using the whole list of peptides found in the mass spectrometric screen as a background, functional annotation of regulated peptides was carried out using the DAVID Bioinformatics Resource. Scansite [33]

(http://scansite.mit.edu/) and PhosphoSitePlus [34] (http://www.phosphosite. org/) were used for the identification of predicted kinases and their identified phosphorylation sites respectively.

3. RESULTS

3.1. Mitogenic Stimulation of PIK3CA & PIK3CB Inducible Cell Lines

MEF β WT cells which have been previously created by retroviral stable transduction of pRXTN rTTA PIK3CB were treated with Adenovirus- and Gesicle-mediated Cre Recombinase (see **2.2.6**) for endogenous p110α and p110β deletions. To characterize p110β-dependent MEF β WT cells, the levels of PI3K downstream proteins were investigated. These results were compared to the p110α-dependent MEF α WT cells which have been created independently by transducing MEF WT cells with a cumate-inducible PIK3CA expressing system.

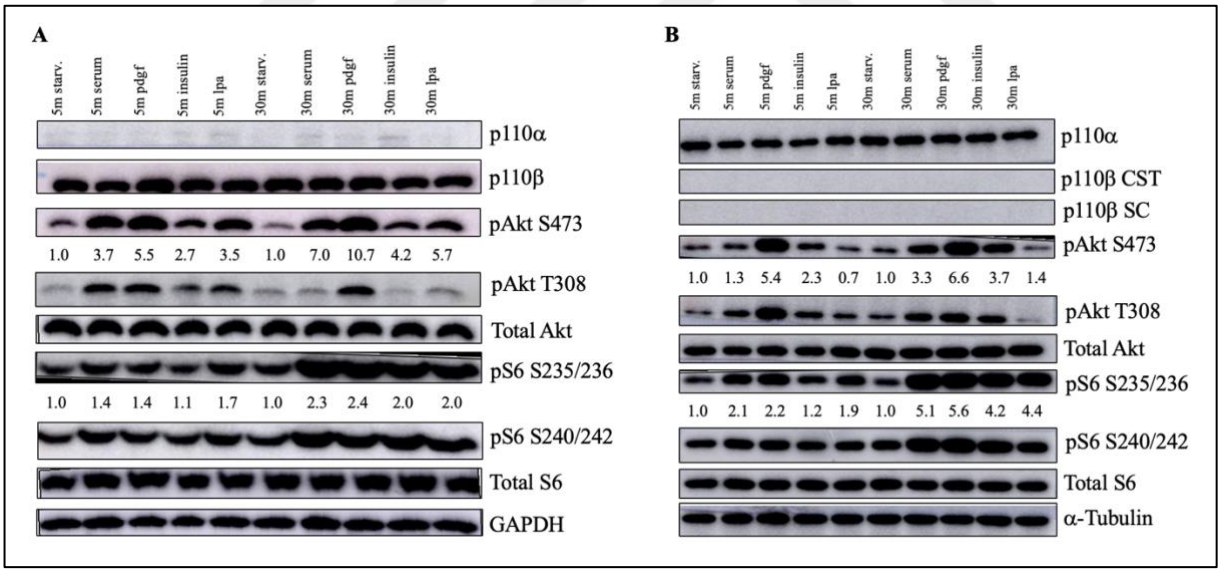

Figure 3.1: Time-dependent response to mitogenic stimuli in β WT and α WT cells. A) β WT cell line **B)** α WT cell line. Cells were starved for 4 h and stimulated with 5% serum, 20 ng/mL PDGF, 2 µg/mL insulin or 20 µM LPA for 5 and 30 mins. p110β levels of human origin (exogenous p110β) in α WT cell line was detected with human-specific CST (Cell Signaling Technology) antibody while SC (Santa Cruz Biotechnology) antibody was used to detect p110β

of both human and mouse origin (exogenous & endogenous). The numbers below the blots represent the relative stimulation group protein levels compared to starvation group and normalized to GAPDH (**Panel A**) or α-Tubulin (**Panel B**). *5m: 5-min stimulation, 30m: 30-min stimulation, starv: starvation.*

After dox and cumate inductions, cells were starved for 4 hours and then PI3K pathway was stimulated with mitogenic stimulators of p110 catalytic subunits. Upon administration of the stimulants, cells were incubated at 37ºC for either 5 or 30 mins. At the end of the stimulation, proteins were extracted according to urea lysis protocol (see **2.2.8.b**). Immunoblotting of the protein samples with p110α and p110β specific antibodies has validated that p110α and p110β levels were depleted in β WT and α WT cells, respectively. p110β levels in α WT cells were checked with 2 different brands of antibodies, Cell Signaling Technologies (CST) and Santa Cruz Biotechnology (SC). As CST recognizes only human p110β protein, it was used to detect proteins derived from the exogenous dox-inducible system with human PIK3CB gene. SC on the other hand, recognizes both human and mouse p110β proteins hence detecting the proteins from both endogenous and exogenous PIK3CB expression systems.

p-Akt and p-S6 specific antibodies have shown increased levels of p-Akt S473/T308 and p-S6 S235/S236/S240/S242 proteins in β WT cells upon serum, PDGF, LPA and insulin stimulations when compared to starvation group (**Figure 3.1**). PDGF was observed as the most potent stimuli in terms of p110β activation with a 10-fold increase in pAkt S473 protein at 30 minutes (**Figure 3.1, A**). Insulin stimulated group however did not show such dramatic fold change as the lowest levels of pAkt S473 was observed although a slight increase still remained when compared to the starvation group. Since insulin activates p110α primarily, this result supports p110β prevalence in β WT cell line. On the other hand, in α WT cells serum, PDGF and insulin stimulations were observed to increase Akt and S6 phosphorylations up to 6-fold

when LPA stimulation failed to cause any significant increase with protein levels similar to the starvation group. This observation also aligns with the function of GPCR stimulating LPA which puts the emphasis on p110β subunit and supports the p110α dependence in α WT cell line. Furthermore, PDGF remained to be the most potent mitogen in terms of p110α activation in α WT cells. It should also be noted that 30 min stimulations caused a dramatic increase in S6 phosphorylation when compared to 5 min stimulations. This proves that PI3K pathway response might vary between early and late response to mitogenic stimulation.

3.2. Downstream Substrate Analysis of PIK3CB Inducible MEF Line

To understand the downstream functional differences between the responses to mitogenic stimuli in β WT cells, protein samples were immunoblotted with antibodies specific for the substrates of phospho-Akt and phospho-PKC (p-PKC). It has been proven before that apart

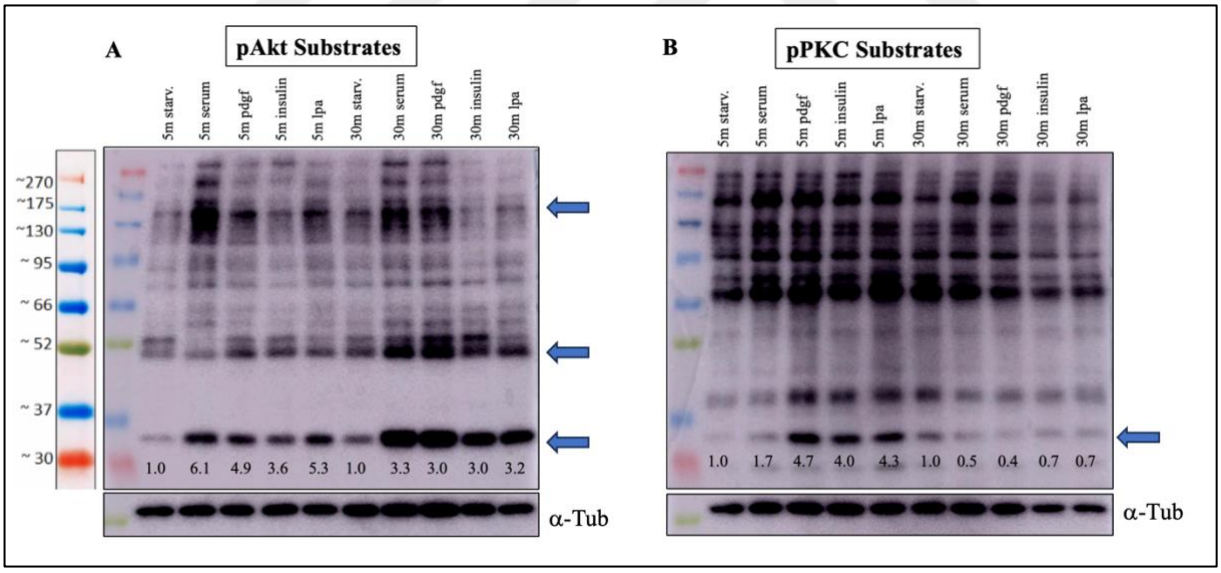

Figure 3.2: Phospho-Akt and Phospho(Ser)-PKC substrate levels in stimulated β WT cells. After cell starvation for 4 h and stimulation with 5% serum, 20 ng/mL PDGF, 2 µg/mL insulin or 20 µM LPA for 5 and 30 mins, protein samples were immunoblotted with **A)** p-Akt (RXXS*/T*) and **B)** p(Ser)-PKC substrate specific antibodies. The numbers below the blots represent the relative stimulation group protein levels compared to starvation group and

normalized to α-Tubulin. *5m: 5-min stimulation, 30m: 30-min stimulation, starv: starvation. α-Tub: α-Tubulin.*

from its stimulation via PI3K pathway, Akt can also be activated in a PI3K-independent manner [35]. α, δ, ζ isoforms of PKC were shown to interact with Akt directly and regulation mechanisms of PI3K/Akt pathway activation by PKCα and PKCζ isoforms have been suggested [36]. Various proteins in the scale of 30-270 kDa were probed upon blotting with p-Akt and p-PKC antibodies (**Figure 3.2**). Three proteins (**Figure 3.2, A; shown with arrows**) in p-Akt substrate blots were observed as distinct bands with different levels at each stimulation condition (**Figure 3.1**). When compared to the starvation group, the protein levels were increased in stimulated cells. This increase was more pronounced for 5-min stimulations.

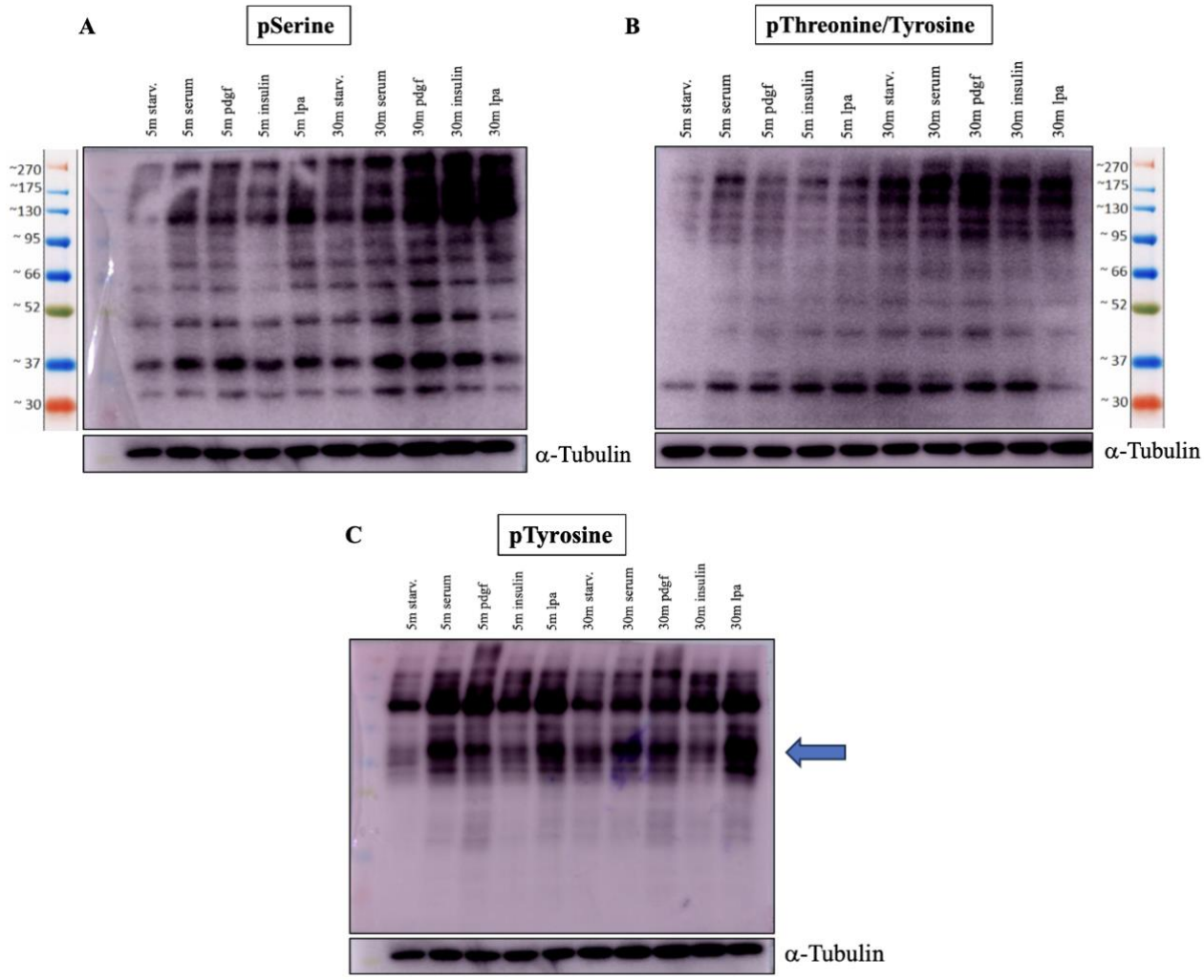

Figure 3.3: p-Serine, p-Threonine/Tyrosine and p-Tyrosine levels in stimulated β WT cells. After cell starvation for 4 h and stimulation with 5% serum, 20 ng/mL PDGF, 2 µg/mL insulin or 20 µM LPA for 5 and 30 mins, protein samples were immunoblotted with **A)** p-Serine, **B)** p-Threonine and **C)** p-Tyrosine residue-specific antibodies. *5m: 5-min stimulation, 30m: 30-min stimulation, starv: starvation.*

Interestingly, the late response levels of the aforementioned protein at 30-37 kDa was less than the early response levels. Insulin stimulation remained to be less potent when compared to the rest of the groups. p-PKC substrate blot also shows most likely the same protein which is seen at 30-37 kDa range in p-Akt substrate blot. The protein levels were again increased at 5 min early response rather than 30 min late response. This suggests that upon mitogenic stimulation, 30-37 kDa protein is phosphorylated by p-Akt and p-PKC right after pathway activation and the half-life of this phosphorylation is relatively short (**Figure 3.2, B**). It should also be noted that the response of p-PKC substrates to different stimuli is the same and independent of p110β prevalence which was previously observed in Akt substrate blot as an increased phosphorylation in cells stimulated with p110β-specific mitogens.

The protein samples were immunoblotted also with antibodies specific for p-Ser, p-Thr/Tyr and p-Tyr residues (**Figure 3.3**). The results have shown that the phosphorylations at serine and threonine residues increase in late-response to stimulation when tyrosine phosphorylations are regulated in a time-independent manner. Rather, the tyrosine residues seem to be sensitive to p110 catalytic domain prevalence (**Figure 3.3, C**). This result suggests that p110β dependent downstream phosphorylations might be regulated through tyrosine residues primarily.

3.3. Mass Spectrometry Analysis of PIK3CB Inducible MEF Line

The samples which were prepared at section **3.1** with urea lysis protocol was sent to Prof. Pedro Cutillas lab for Mass Spectrometry (MS) analysis. Cells were starved for 4 hours and then stimulated with serum or other mitogens such as PDGF, Insulin and LPA for either 5- or 30-minutes. Including the starved control group, 10 samples were prepared in total with 3 replicates for each. 750 µg lysate from each sample was sent for LC-MS/MS analysis. The phosphoproteome of each stimulation group was compared to the starved group. The results have yielded various phosphoproteins which were up/down-regulated at late and early response to stimuli. Proteins that have a fold change of 1.5 or more were selected for further analysis. These proteins and their interaction network were displayed STRING database (**Figure 3.4**) [37]. Some of them were found to be differentially regulated in multiple stimulation groups when some were specific to the stimuli. They were also compared to the MS results of α WT cell line and most proteins were found to be specific to β WT line. The ones that were found in both cell lines were indicated with *star* symbol on **Figure 3.4**.

Aligning with the immunoblot results (**Figure 3.1**), insulin-specific phosphoproteins were found to be scarce when serum and PDGF-specific proteins were quite abundant. The number of LPA-specific proteins were elevated in early response downregulated group. Some phosphoproteins were common in two or three stimulation groups. Ribosomal protein S6 was among those which were repeated in three different groups (serum, PDGF and insulin) and it was observed as a late response upregulated phosphoprotein. It was found to be phosphorylated in common Akt and mTOR target residues S235/236, in addition to S240/242 and T241.

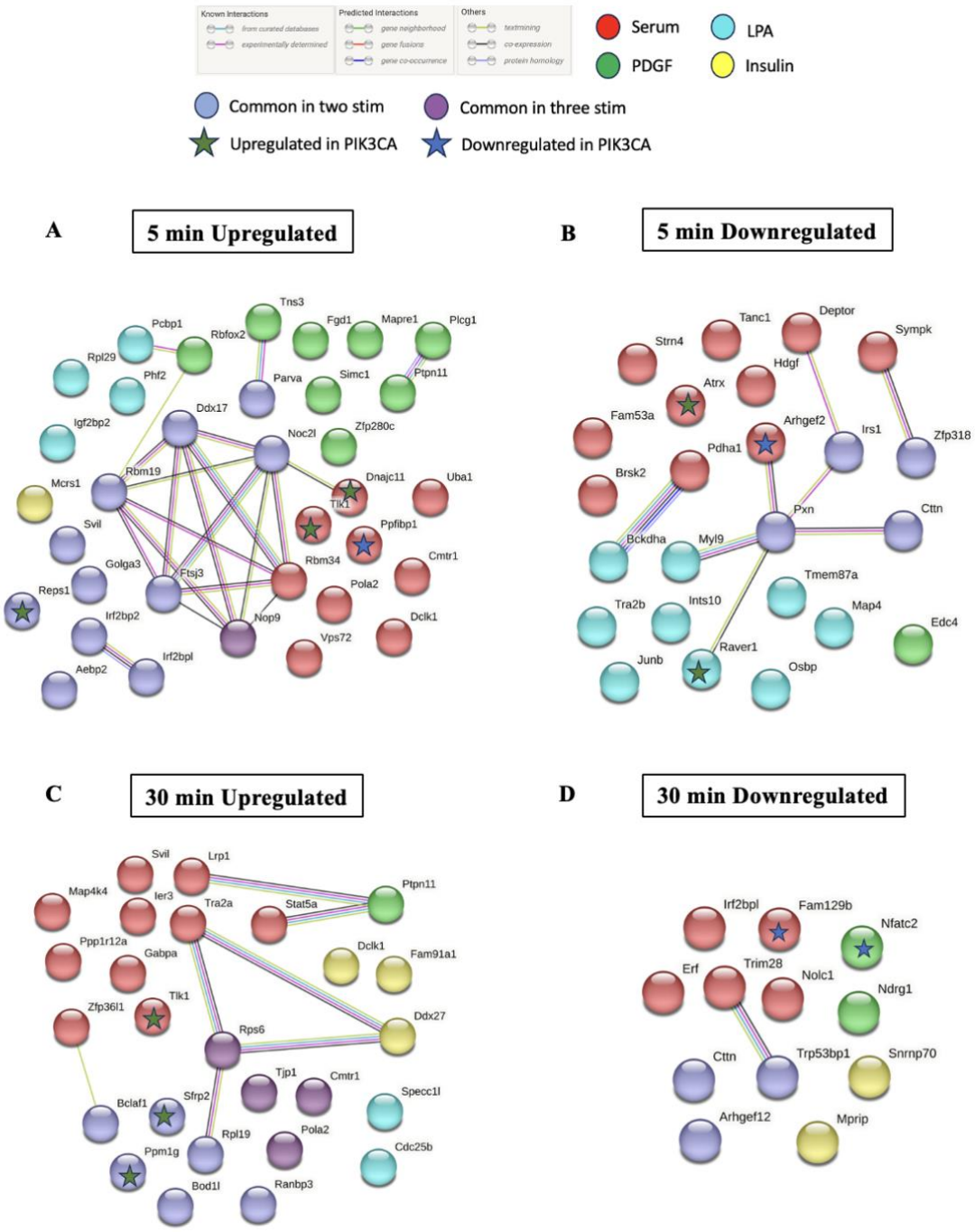

Figure 3.4: Interaction networks between up/down-regulated phosphoproteins in stimulated β WT cells. STRING interaction analysis was conducted for up/down-regulated early (**A & B,** 5 min stimulations) and late response (**C & D**, 30 min stimulations) phosphoproteins found in MS analysis. Proteins specific to stimuli and those which were repeated in multiple stimulation groups were colour coded. Green and blue stars indicate proteins found also in the MS analysis of α WT cells.

This observation supports the immunoblot results as S6 levels were found to be increased 2-fold in 30-min stimulation groups. Some other previously reported Akt and mTOR substrates were also encountered in the MS results of different stimulation groups: Plcg1 Y1253 and Golga3 S1479 in early response upregulated group; Irs1 T1099 & S24/M2 and Deptor S238 in early response downregulated group; Cdc25b S351 in late response upregulated group and Trim28 S683 in late response downregulated group.

A protein network of Ddx17, Rbm19, Ftsj3, Rbm34, Noc2l and Nop9 associated with transcriptional regulation and RNA binding was found in early response upregulated group (**Figure 3.4, A**). g:Profiler [38] analysis has also shown functional enrichment in transcriptional coregulator activity along with binding activity (**Figure 3.5, A**). Proteins in this group are mostly abundant in the nuclear compartments which supports the transcriptional regulation activity. Some proteins associated with cellular signaling such as Reps1 and Ptpn11 were among the early response upregulated group along with few which takes part in cell migration (Svil, Plcg1) and cytoskeletal rearrangement (Mapre1, Fgd1, Parva). On the other hand, the downregulated early response proteins were dominantly associated with structural functions (**Figure 3.5, B**). Cytoskeletal protein binding was especially distinctive for this group with a protein network including cytoskeletal proteins such as Pxn and Cttn. Along with Cttn, Arhgef2, Sympk and Myl9 were observed in relation to tight junctions. Microtubule-associated protein Map4 was also among early response downregulated phosphoproteins. Interestingly, Pdha1 and Bckdha were found to be interacting and associated with oxidoreductase activity.

Late response upregulated phosphoproteins were found to be abundant in the nucleus and most were observed to be associated with nuclear lumen **(Figure 3.6, A)**. Nucleocytoplasmic transport was also enhanced for this group with proteins Pola2, Ier3, Ranbp3, Ptpn11 and Ppp1r12a. Functional enrichment was also indicated for protein

A

5 min Upregulated

GO:MF		stats
Term name	Term ID	p_{adj}
transcription coregulator activity	GO:0003712	7.262×10^{-4}
binding	GO:0005488	5.794×10^{-3}
transcription corepressor activity	GO:0003714	3.106×10^{-2}

1 to 3 of 3 Page 1 of 1

GO:BP		stats
Term name	Term ID	p_{adj}
transcription initiation-coupled chromatin remodeling	GO:0045815	1.732×10^{-2}

1 to 1 of 1 Page 1 of 1

GO:CC		stats
Term name	Term ID	p_{adj}
nucleoplasm	GO:0005654	2.427×10^{-6}
nuclear lumen	GO:0031981	4.259×10^{-4}
nucleus	GO:0005634	7.116×10^{-4}
organelle	GO:0043226	1.184×10^{-3}
chromosome	GO:0005694	8.237×10^{-3}
intracellular anatomical structure	GO:0005622	1.086×10^{-2}
preribosome, small subunit precursor	GO:0030688	2.669×10^{-2}
anchoring junction	GO:0070161	4.911×10^{-2}
nuclear speck	GO:0016607	4.975×10^{-2}

1 to 9 of 9 Page 1 of 1

B

5 min Downregulated

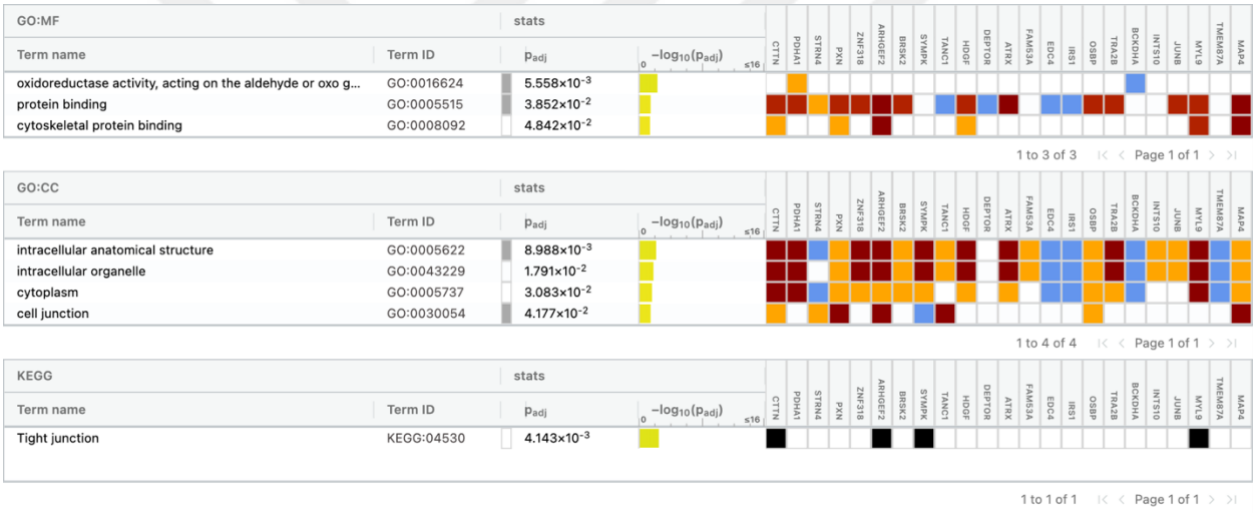

GO:MF		stats
Term name	Term ID	p_{adj}
oxidoreductase activity, acting on the aldehyde or oxo g...	GO:0016624	5.558×10^{-3}
protein binding	GO:0005515	3.852×10^{-2}
cytoskeletal protein binding	GO:0008092	4.842×10^{-2}

1 to 3 of 3 Page 1 of 1

GO:CC		stats
Term name	Term ID	p_{adj}
intracellular anatomical structure	GO:0005622	8.988×10^{-3}
intracellular organelle	GO:0043229	1.791×10^{-2}
cytoplasm	GO:0005737	3.083×10^{-2}
cell junction	GO:0030054	4.177×10^{-2}

1 to 4 of 4 Page 1 of 1

KEGG		stats
Term name	Term ID	p_{adj}
Tight junction	KEGG:04530	4.143×10^{-3}

1 to 1 of 1 Page 1 of 1

Gene Ontology
- Inferred from experiment [IDA, IPI, IMP, IGI, IEP]
- Direct assay [IDA], Mutant phenotype [IMP]
- Genetic interaction [IGI], Physical interaction [IPI]
- Inferred from High Throughput Experiment [HDA, HMP, HGI, HEP]
- High Throughput Direct Assay [HDA], High Throughput Mutant Phenotype [HMP]
- High Throughput Genetic interaction [HGI], High Throughput Expression pattern [HEP]
- Traceable author [TAS], Non-traceable author [NAS], Inferred by curator [IC]
- Expression pattern [IEP], Sequence or structural similarity [ISS], Genomic context [IGC]
- Sequence Model [ISM], Sequence Alignment [ISA], Sequence Orthology [ISO]
- Biological aspect of ancestor [IBA], Rapid divergence [IRD]
- Reviewed computational analysis [RCA], Electronic annotation [IEA]
- No biological data [ND], Not annotated or not in background [NA]

Biological pathways
- KEGG , Reactome

Regulatory motifs in DNA
- TRANSFAC TFBS , miRTarBase

Human Protein Atlas
- [Enhanced, Supported, Approved]

CORUM protein complexes
- CORUM

Human Phenotype Ontology
- Human Phenotype Ontology (sequence homologs in other species)

The colors for log scale:

0 5 10 15 20 25 30 35 40 45 ≤50

Figure 3.5: Functional enrichment analysis of early response phosphoproteins in stimulated β WT cells. g:Profiler analysis was conducted for **A)** upregulated **B)** downregulated early response (5 min stimulation) phosphoproteins found in MS analysis.

dephosphorylation and phosphatase activity by g:Profiler analysis; proteins Cdc25b, Ppp1r12a, Ppm1g and Ptpn11 were involved in these processes. Proteins such as RpS6, Tlk1, Zfp36l1, Svil, Stat5a, Ier3 were found to be involved in cell cycle and nearly all proteins in this group were associated with intracellular anatomical structure. An interaction network was identified between RpS6, Tra2a and Ddx27 (**Figure 3.4, C**). An apoptosis-related protein Bclaf1 was also identified among this group. Ptpn11 Y546 & T547 and Tlk1 S20/T21 phosphoproteins were common with the early response upregulated group. Late response downregulated phosphoproteins on the other hand, were abundant in the nucleoplasm and regulation of cellular metabolic processes including RNA metabolism were enriched in this group (**Figure 3.6, B**). Trim28, Irf2bpl, Nolc1, Tp53bp1, Nfatc2 and Snrnp70 were matched with RNA metabolism function when Erf, Cttn and Mprip were added on for cellular metabolism. No previously reported LPA-specific proteins were identified for this group (**Figure 3.4, D**).

3.4. PI3K Pathway Activation in PIK3CB E1051K & N553S Mutant MEF Lines

To understand how PI3K pathway is activated due to PIK3CB E1051K (EK) kinase domain and N553S (NS) regulatory domain mutations, dox-inducible MEF β EK and β NS lines were created by retroviral transduction of pRXTN rtTA PIK3CB E1051K or N553S vectors (see **2.2.4 & 2.2.5**). The endogenous wildtype PIK3CB and PIK3CA were deleted with Adenovirus- and Gesicle-mediated Cre Recombinase treatments. Upon transduction, the mutant cells were observed to grow much more rapidly when compared to the WT cell lines. Also, the typical

MEF morphology of β EK cells was observed to be different than WT cells. EK cells were smaller in size and the spindles common for MEF cells were less apparent (**Figure 3.7**).

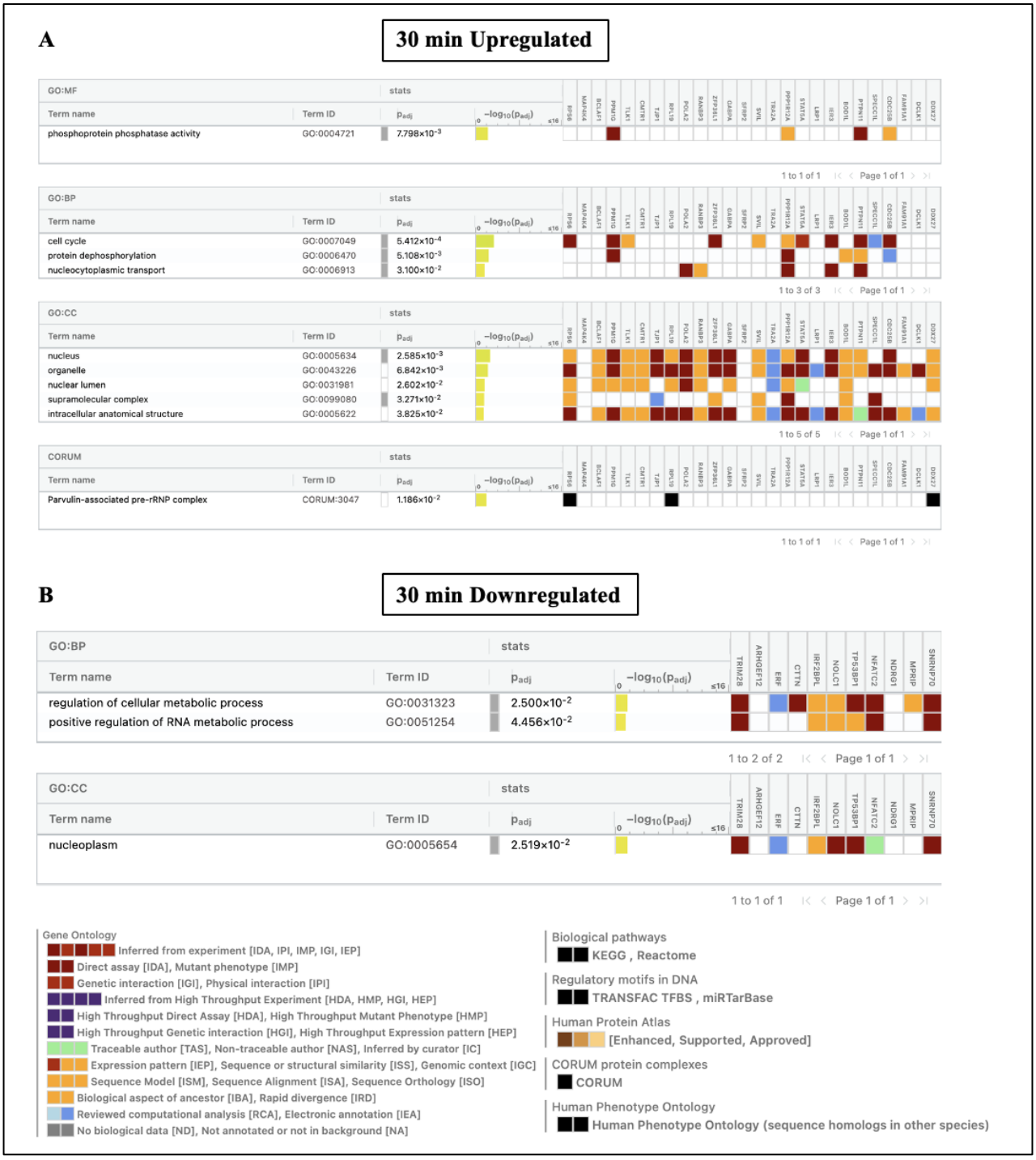

Figure 3.6: Functional enrichment analysis of late response phosphoproteins in stimulated β WT cells. g:Profiler analysis was conducted for **A)** upregulated **B)** downregulated late response (30 min stimulation) phosphoproteins found in MS analysis.

The increase in proliferation rate of β mutants was quantified as percent viability after SRB proliferation assay was performed (see **2.2.12**). β WT, EK & NS cells were cultivated with either KIN193, a selective p110β inhibitor, or 2% serum (**Figure 3.8, A**). β EK and NS cells grew drastically faster than β WT cells. No significant difference of growth was observed between day 2 and day 3 for WT cells **(Figure 3.8, B)**. The percent cell viability graphs have shown that KIN193 has significantly decreased the proliferation rate of WT and NS cells to 50-60%, similar to the effect of serum-depleted media. EK cells on the other hand have resisted the effects of KIN193 treatment at day 2, conserving the viability percentage at 75%, although its proliferation rate was decreased to 50% in serum-depleted condition **(Figure 3.9, A)**. These results prove that the growth advantage of E1051K mutant is independent of the mechanism by which KIN193 inhibits p110β. Accordingly, it can be stated that the catalytic domain PIK3CB mutants might confer resistance to isoform-specific catalytic domain inhibitors.

To understand the growth dependences of mutant lines along PI3K axis in more depth, another SRB proliferation assay was conducted with various inhibitors against some PI3K downstream effectors: Akt inhibitor MK2206, mTORC1 inhibitor RAD001 (Everolimus) and Rac1 inhibitor EHT1864 (**Figure 3.10**). From day 2 to day 3, a significant difference between the growth rates of WT line and the mutants has been observed once again for DMSO vehicle control in 8% serum media (**Figure 3.10, B)**. The cell viability percentages after inhibitor treatment have shown that at day 2, the cell proliferation starts decreasing for all cell lines (**Figure 3.11**). RAD001 and EHT1864 treatments have decreased the viability to 50% and 65% respectively. Although RAD001 and EHT1864 affect all lines similarly, MK2206 seems to be less effective on the WT cells. Cell viability for WT line was more than 65% percent when it was decreased to 50% for mutant lines. Overall, EHT1864 was found to be the least effective

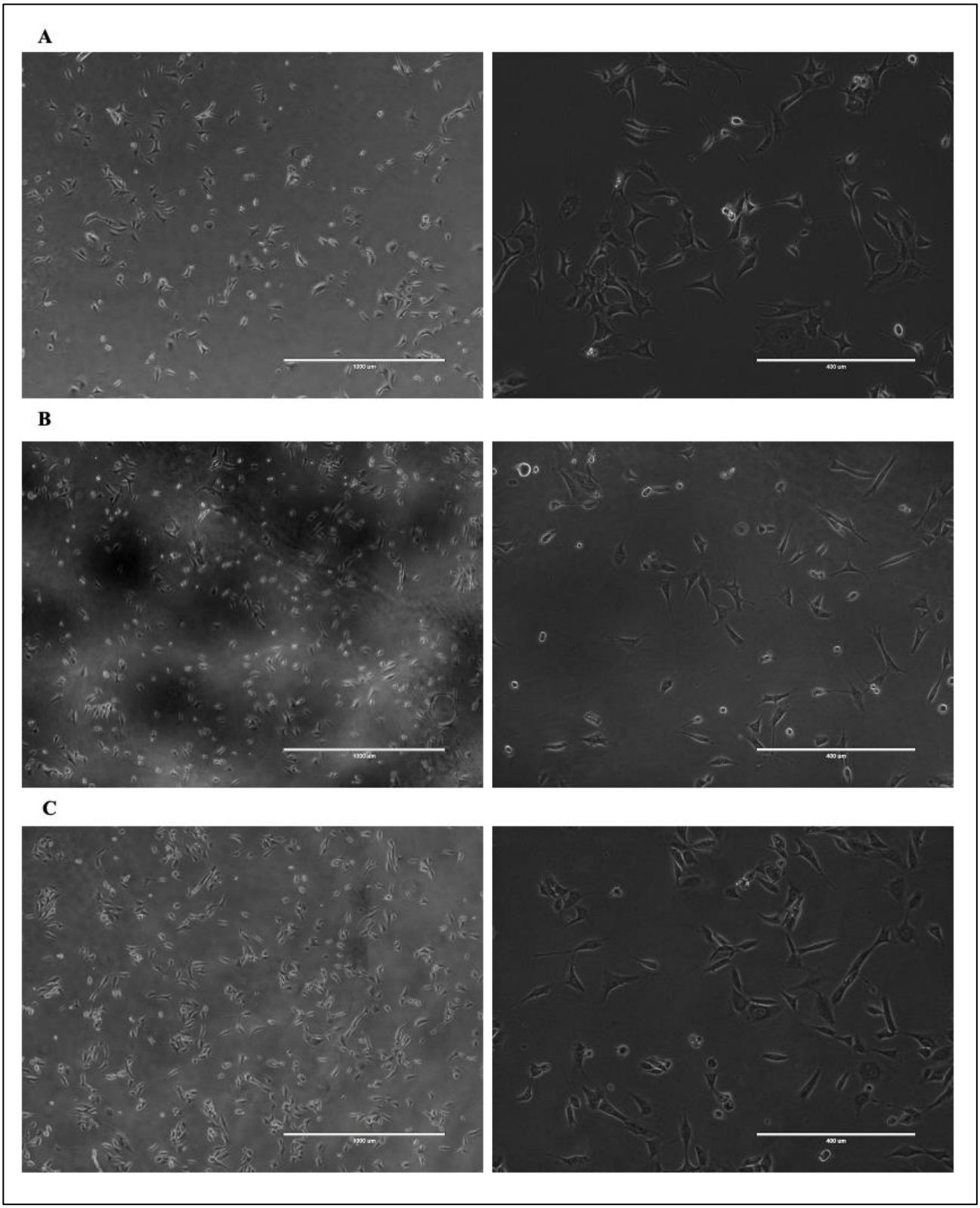

Figure 3.7: β WT, EK & NS cell morphologies under phase contrast microscope. β WT (**A**), EK (**B**) and NS (**C**) cells were cultivated for 2 days at maintenance conditions and visualized with phase contrast microscope under 4x (left) and 10x (right) magnification.

on the growth of the mutant lines when RAD001 was the most potent as it decreased the proliferation of all lines 50% after 2 days of treatment. These results indicate that the proliferative advantage of the mutants is dependent more on Akt and mTORC1 activity downstream of PI3K rather than Rac1.

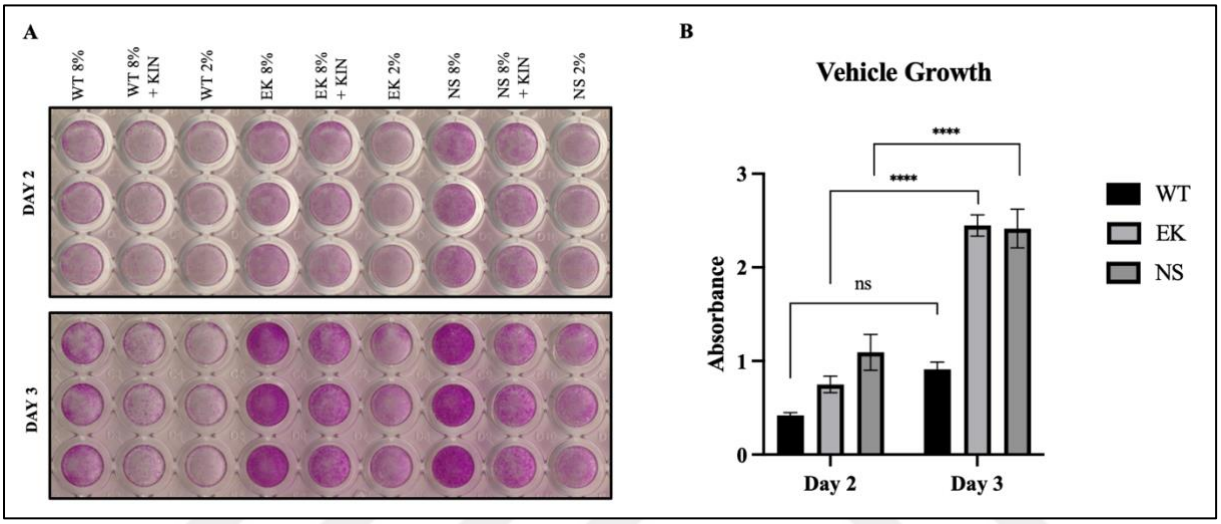

Figure 3.8: SRB proliferation assay with KIN193 treated β WT, EK & NS cells. A) 100 cells per well were seeded on 96-well plates and grown for 3 days with either 8% serum media, 2 μM KIN193 in 8% serum media or 2% serum media. B) Absorbance at 564 nm was measured at day 2 and day 3. The growth under regular maintenance conditions (8% serum) with DMSO vehicle was graphed. Statistical significance was tested with two-way ANOVA. Error bars indicate SEM of three independent biological replicates (*n=3, * p<0.05, ** p<0.01, *** p<0.001*).

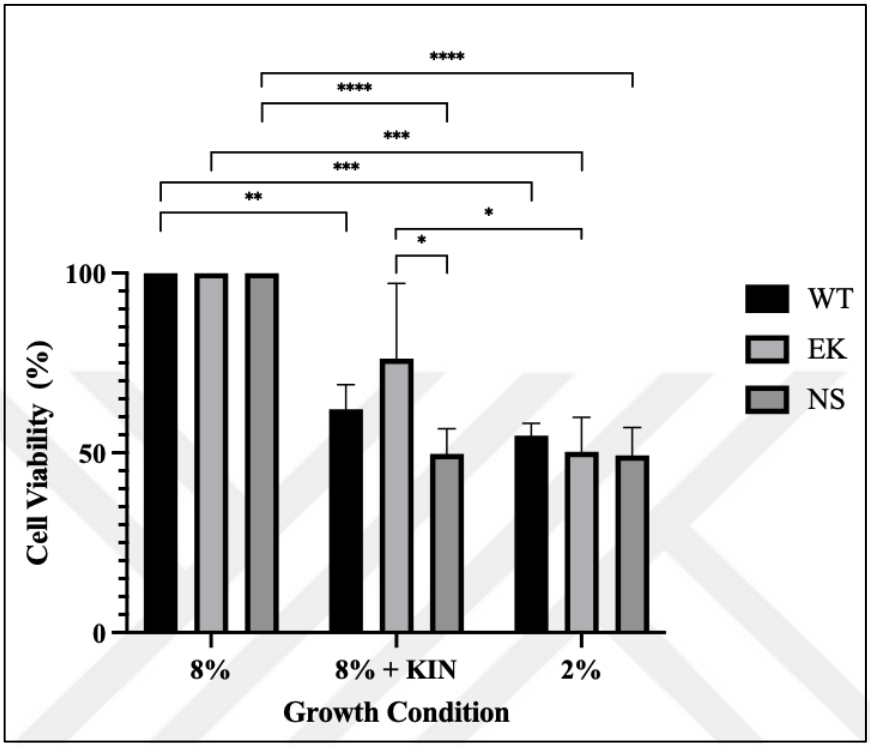

Figure 3.9: Viability percentage of β WT, EK & NS cells upon KIN193 treatment. For normalization, the absorbance value of background control was subtracted from each DMSO vehicle and treatment group measurement. The normalized mean absorbance values of the treatment groups were divided by the mean absorbance for vehicle 8% group and multiplied by 100% to obtain percentage of cell viability at two days after the administration of KIN193 or 2% serum media. Statistical significance was tested with two-way ANOVA. Error bars indicate SEM of three independent biological replicates (*n=3, * p<0.05, ** p<0.01, *** p<0.001).*

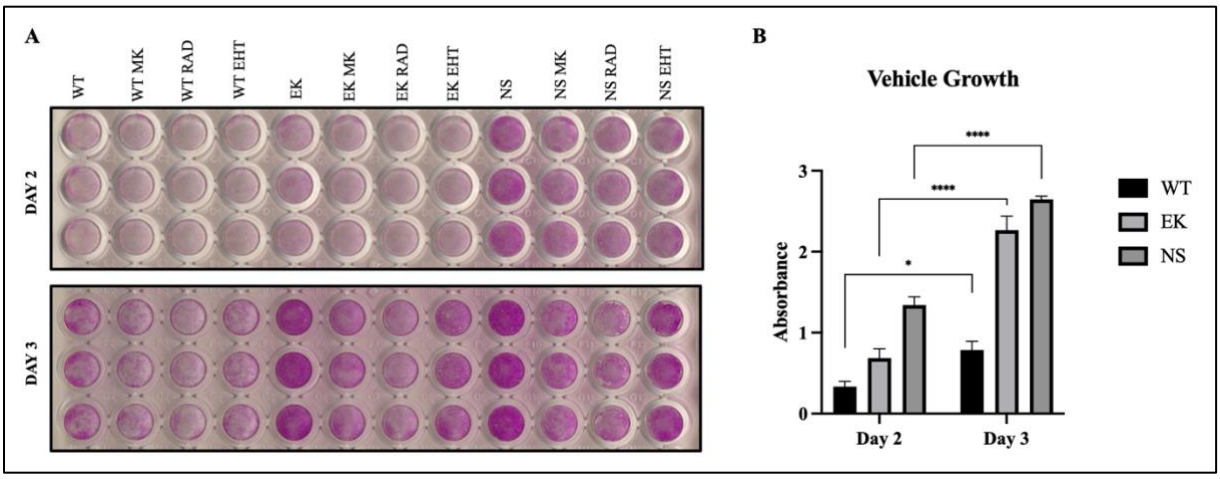

Figure 3.10: SRB proliferation assay with inhibitor treated β WT, EK & NS cells. A) 100 cells per well were seeded on 96-well plates and grown for 3 days with either 8% serum media, 2% serum media, or 1 µM MK2206, 200 nM RAD001 and 5 µM EHT1864 in 8% serum media or. B) Absorbance at 564 nm was measured at day 2 and day 3. The growth under regular maintenance conditions (8% serum) with DMSO vehicle was graphed. Statistical significance was tested with two-way ANOVA. Error bars indicate SEM of three independent biological replicates (*n=3, * p<0.05, ** p<0.01, *** p<0.001*).

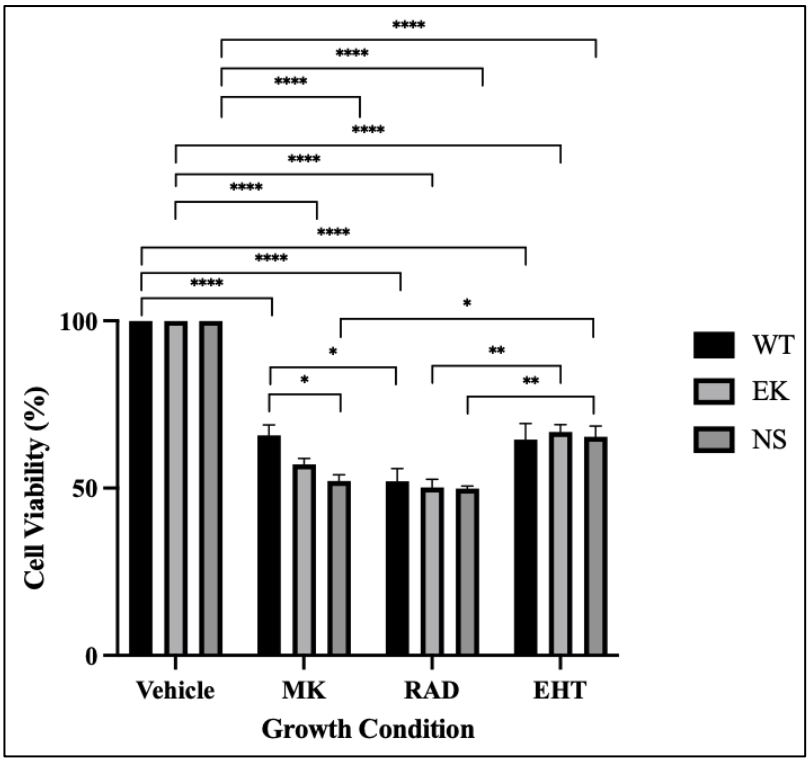

Figure 3.11: Viability percentage of β WT, EK & NS cells upon inhibitor treatment. For normalization, the absorbance value of background control was subtracted from each DMSO vehicle and treatment group measurement. The normalized mean absorbance values of the treatment groups were then divided by the mean absorbance for vehicle group and multiplied by 100% to obtain percentage of cell viability at two days after the administration of inhibitors. Statistical significance was tested with two-way ANOVA. Error bars indicate SEM of three independent biological replicates (*n=3, * p<0.05, ** p<0.01, *** p<0.001*).

To show that the proliferative advantage of the mutants is connected to the overactivation of PI3K pathway, biochemical analysis of the downstream proteins was conducted. After serum-deprivation and dox-induction, proteins were extracted from β WT, EK & NS cells according to urea lysis protocol (see **2.2.8.b**). Immunoblotting results have shown that p110β levels in β EK and β NS lines were elevated upon transduction when compared to MEF WT and β WT (**Figure 3.12**).

pAkt S473 levels were increased 8-fold in β EK & NS lines when compared to the WT line. Although β WT line also shows increased pAkt levels relative to WT line, the fold change only goes up to 5-to-6-fold which stays below the level of change in mutant lines. pS6 levels were also elevated 2-to-3-fold in mutant lines and in β WT line. These results prove that PI3K downstream pathway activation is enhanced not only in E1051K and N553S mutants but also in cells with wildtype p110β amplification.

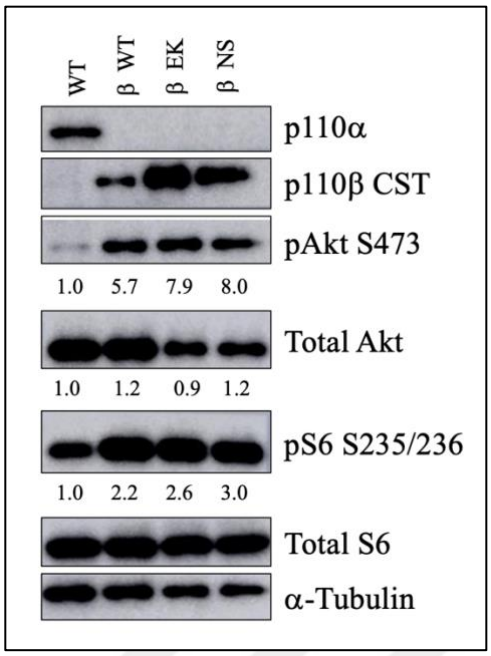

Figure 3.12: PI3K downstream phosphoprotein levels in MEF β EK and β NS mutant cells. Cells were cultured in 2% FBS (tet-free) media for 2 days prior to harvest to eliminate serum-induced phosphorylations. 0.7 ug/mL dox was administered with 2% media to the inducible PIK3CB lines. The numbers below the blots represent the relative protein levels compared to WT group and normalized to α-Tubulin.

3.5. Downstream Substrate Analysis of PIK3CB E1051K & N553S Mutant Cell Lines

The downstream pAkt and pPKC substrates of β EK & NS protein samples were analysed in comparison to WT and β wt lines. In WT cell line fewer number of substrate proteins were observed and the banding pattern on the immunoblot membranes were much different from the β lines (**Figure 3.13**). A distinct band between 30-37 kDa (shown with an arrow) similar to the one in **Figure 3.2** was again visible on both pAkt and pPKC substrates blots. The levels of this protein were increased in mutants up to 9-fold. To estimate the phosphorylation residues that are frequently modified in mutant cells, protein samples were probed with p-Ser, p-Thr/Tyr and

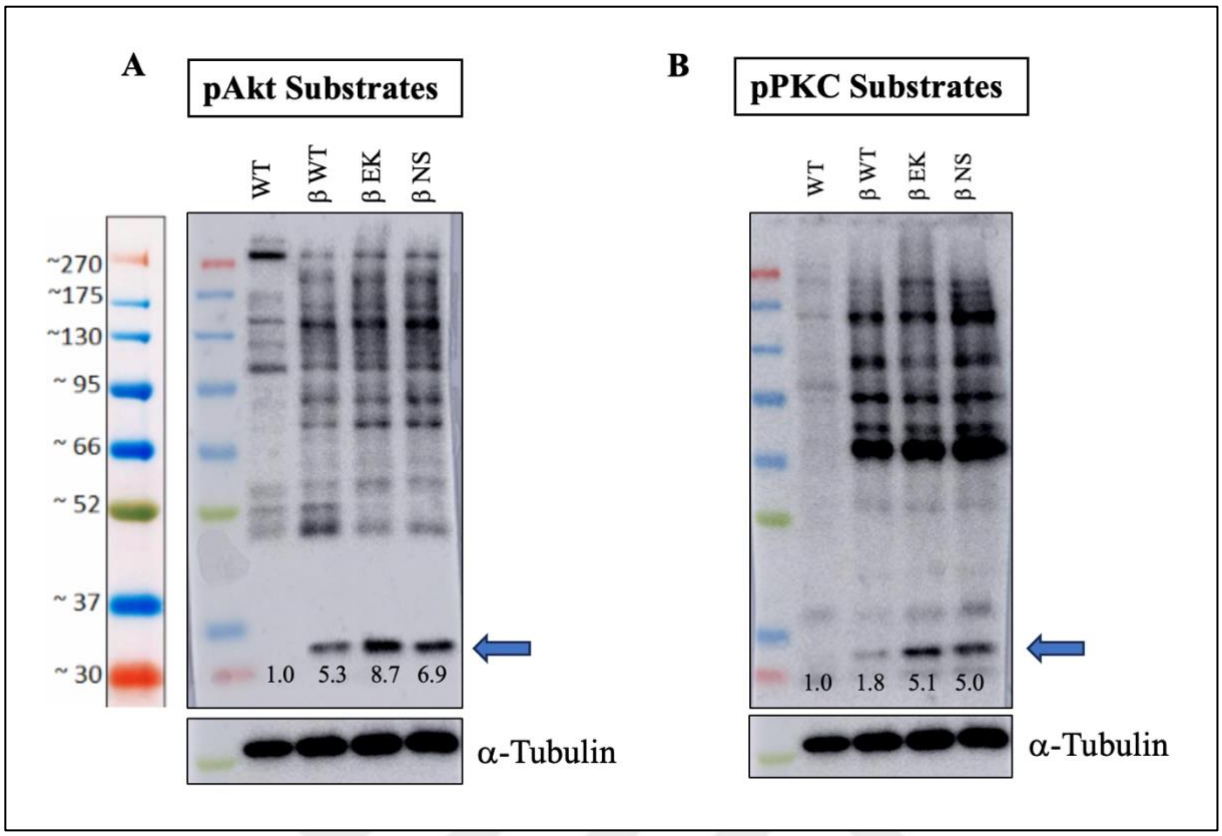

Figure 3.13: Phospho-Akt and Phospho(Ser)-PKC substrate levels in β EK & NS cells. Cells were cultured in 2% FBS (tet-free) media for 2 days prior to harvest to eliminate serum-induced phosphorylations. 0.7 ug/mL dox was administered with 2% media to the inducible PIK3CB lines. The numbers below the blots represent the relative protein levels compared to WT group and normalized to α-Tubulin.

p-Tyr specific antibodies (**Figure 3.14**). For all phospho-residues, β lines again displayed different banding patterns than the WT line. All β lines were observed to have similar proteins phosphorylated on Ser residues (**Figure 3.14, A**). Ser and Tyr phosphorylations of some proteins were amplified in β WT line when compared to the mutant lines (**Figure 3.14, C**). Thr phosphorylations on the other hand, were enhanced mostly in the mutant lines (**Figure 3.14, B)**. This result might suggest that in p110β E1051K and N553S mutants PI3K downstream pathway activation is mostly regulated through activating Thr and inhibiting Ser/Tyr phosphorylations.

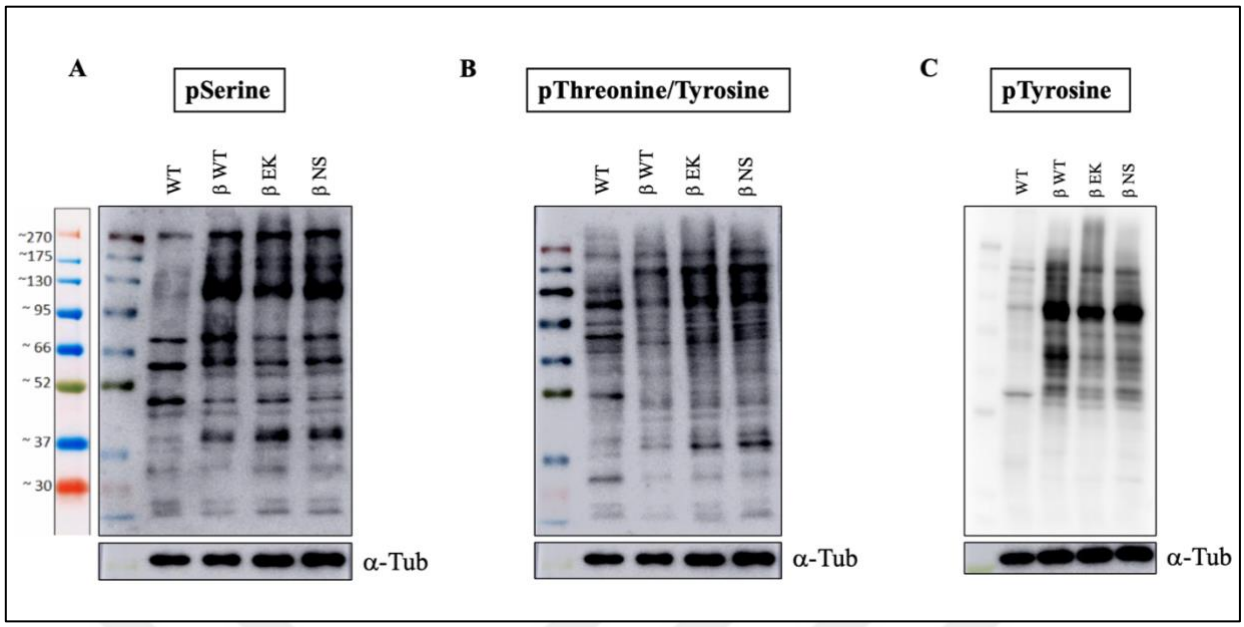

Figure 3.14: p-Serine, p-Threonine/Tyrosine and p-Tyrosine levels in β EK & NS cells. Cells were cultured in 2% FBS (tet-free) media for 2 days prior to harvest to eliminate serum-induced phosphorylations. 0.7 ug/mL dox was administered with 2% media to the inducible PIK3CB lines. *α-Tub: α-Tubulin.*

The 30-37 kDa protein band which was identified as a p-Akt substrate in all β WT, EK & NS cell lines, was found at close distance to a common Akt1 & Akt2 substrate ribosomal protein S6. To figure out if the band observed in p-Akt Substrates blots (**Figures 3.2 & 3.13**), was the canonical 32 kDa pS6, β WT cells were starved for 4 hours, stimulated with 10% serum for 30 mins and proteins were isolated with NP-40 lysis (**see 2.2.8.c**). After protein samples were conjugated with p-Akt Substrates antibodies, they were immunoprecipitated with A/G agarose beads (**see 2.2.11**). The antibody-protein elute was then co-immunoprecipitated with pS6 S235/S236 antibody or proline-rich Akt substrate of 40 kDa (PRAS40) antibody as positive control. Western blot results have shown that in serum stimulated cells PRAS40 immunoprecipitated with p-Akt Substrates antibody as expected, when pS6 S235/S236 did not (**Figure 3.15**).

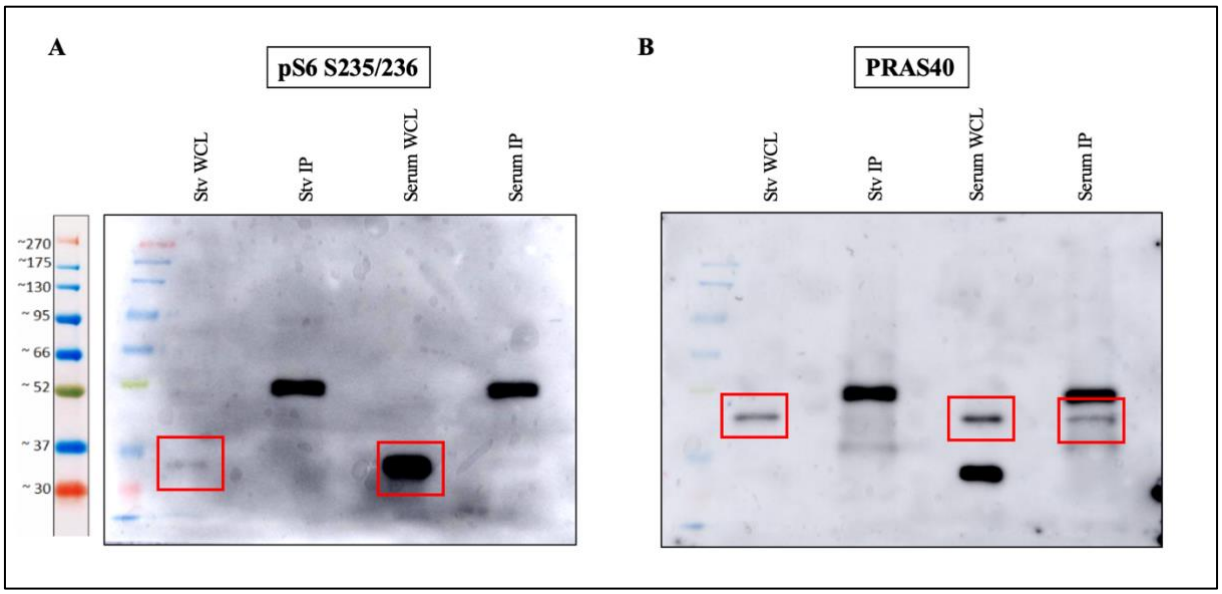

Figure 3.15: pS6 does not co-immunoprecipitate with pAkt Substrates. pAkt Substrates antibody conjugated protein samples of 10% serum stimulated p110β WT cells were immunoprecipitated with agarose beads. The elute was co-immunoprecipitated with either pS6 S235/236 or PRAS40 antibodies. Red rectangles indicate the corresponding blots. *Stv WCL: Starvation whole cell lysate; Stv IP: Starvation immunoprecipitated; Serum WCL: Serum whole cell lysate; Serum IP: Serum immunoprecipitated.*

These results indicate that the protein identified as a PI3K downstream Akt substrate in β cell lines is not a canonical pS6 protein. Instead, it might be a novel PI3K downstream effector.

3.6. Mass Spectrometry Analysis of PIK3CB E1051K & N553S Mutant MEF Lines

The samples which were prepared at **3.1** with urea lysis protocol was sent to Prof. Pedro Cutillas lab for Mass Spectrometry (MS) analysis. Cells were maintained with 2% FBS (tet-free) media for 2 days prior to harvest to eliminate serum-induced phosphorylations. 0.7 ug/mL dox was administered with 2% media to the inducible PIK3CB lines. Including the β WT control group, 3 samples were prepared in total with 3 replicates for each. 750 µg lysate from each sample was sent for LC-MS/MS analysis. The phosphoproteome of each mutant was compared to the β WT line and also to each other. Proteins that have a fold change of 1.5 or

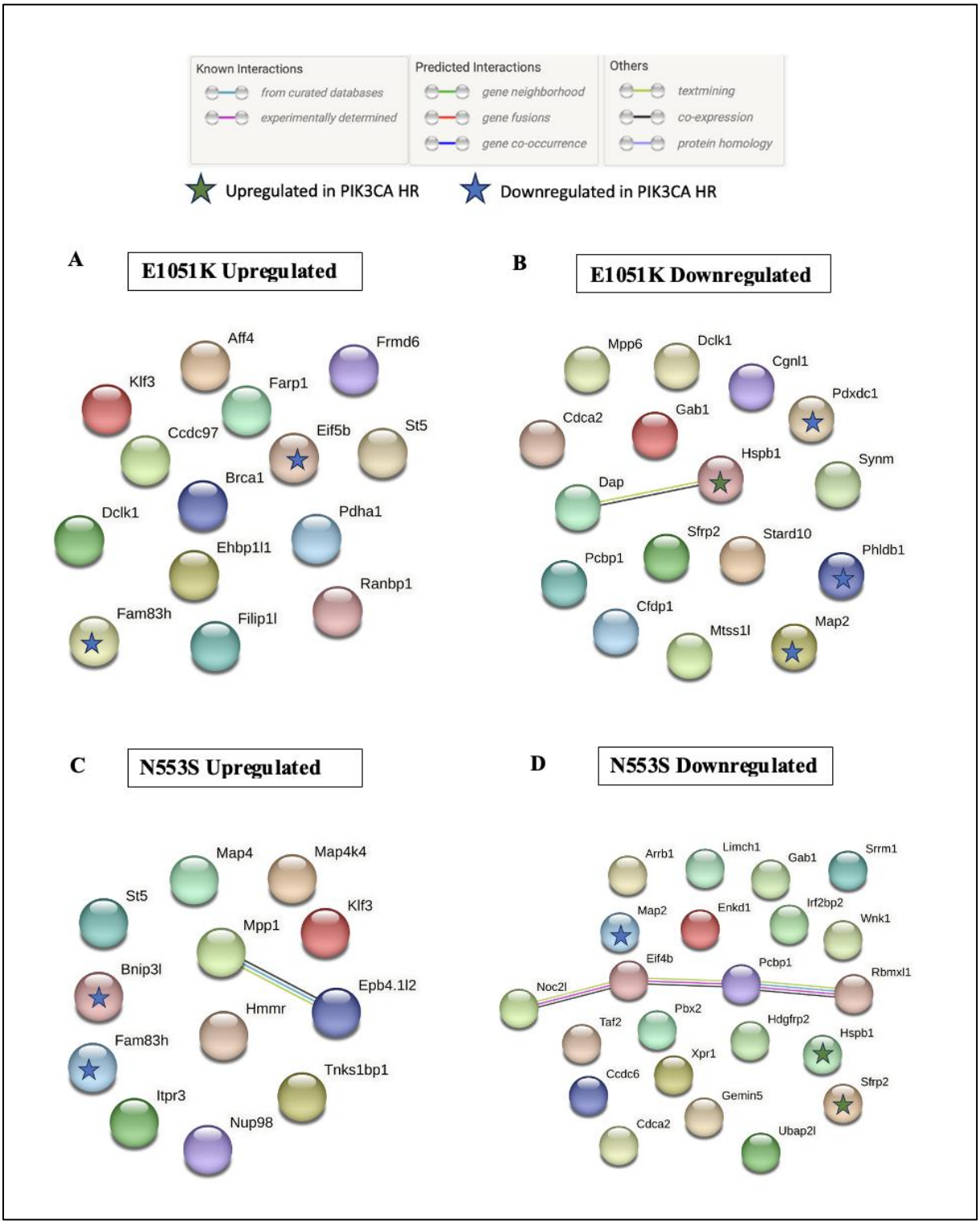

Figure 3.16: Interaction networks between up/down-regulated phosphoproteins in β EK & NS cells. STRING interaction analysis was conducted for up/down-regulated phosphoproteins found in MS analysis of E1051K (**A & B**) and N553S (**C & D**) mutant cells. Green and blue stars indicate proteins found also in the MS analysis of α cells.

more were selected for the bioinformatics study. STRING and g:Profiler analysis were conducted to portray the interaction network among the phosphoproteins and their enriched functions. There were some noteworthy Akt and mTOR substrates found in the phosphoproteome of the mutants: Brca1 (S504), Phldb1 (S445), Dap (S60), Gab1 (S418), Nup98 (S653), Map4 (S766), Itpr3 (M2668, S2669), Wnk1 (S165), Eif4b (S445/T461) and Srrm1 (S672). These were taken as positive controls of the mutant MS analysis.

STRING network of the upregulated proteins in E1051K mutant has shown that there are no identified interactions between these proteins (**Figure 3.16**). Proteins such as Brca1, Dclk1, Farp1 and Ranbp1 were associated with cytoskeletal organization (**Figure 3.17**). The tumor suppressor Brca1 was also observed related to DNA repair. A tumorigenicity-associated protein St5 was also found to be upregulated along with a tumor suppressor Filip1. Among the downregulated proteins, Hspb1 (stress resistance and actin organization) and Dap (negative regulator of autophagy) were identified as interactors. Along with Hspb1, proteins Gab1, Sfrp2, Map2, Cfdp1 and Phldp1 were associated with regulation of anatomical structure morphogenesis which aligns with the morphological changes observed in **Figure 3.7**. Gab1 was also involved in VEGF-induced cell migration and nucleic-acid binding protein Pcbp1 was related to cellular metabolism. Most of these proteins were abundant in cytoplasm and cell junctions (**Figure 3.17**).

The analysis of N553S mutant has proved that the cellular effects of this regulatory subunit mutant are different than those of E1051K, the catalytic subunit mutant. The upregulated phosphoproteins in N553S mutant were abundant in the intracellular organelles and cytoskeleton **(Figure 3.18)**. Proteins such as Map4 and Fam83h associated with microtubule assembly and structural organization. Bnip3, an apoptotic inducer, and Nup98, a nuclear pore complex protein, were also identified. The downregulated phosphoproteins on the other hand

were found to be involved in transcriptional regulation, cellular signaling and metabolism. Various mechanisms of transcriptional regulation were found related: A histone acetyltransferase inhibitor Noc2l was associated with transcriptional repression along with a transcriptional corepressor Irfbp2 which is independent of histone deacetylase activity. Proteins such as Gab1, Sfrp2 and Arrb1 were observed in the context of cellular signaling and metabolism. Also, an RNA-binding protein Rbmxl1 was identified with a possible involvement in pre-mRNA splicing. It should also be noted that RNA metabolism function was highlighted with the proteins Eif4b, Pcbp1, Gemin5 and Hspb1 **(Figure 3.18)**. STRING analysis has shown Pcbp1 interacting with Eif4b and Rbmxl1. Eif4b was also found interacting with Noc2l (**Figure 3.16**).

The proteins identified in Mass Spectrometry was checked for their molecular weights to see if there are any that lies between 30-37 kDa range. Such proteins might be candidates of Akt substrates which align with the band observed in **Figure 3.2** and **Figure 3.13**. Although this band can correspond to as yet unidentified Akt substrate, Pcbp1 (37 kDa) and Sfrp2 (33 kDa) were candidates found from literature which lay between 30-37 kDa range. The kinase motifs on these proteins were analyzed on SCANSITE 4.0 [33] and a basophilic serine/threonine Akt kinase motif was observed for Pcbp1 at site T180. On the other hand, the MS results have shown that Pcbp1 was downregulated with a fold change of -1.5 in β EK cells and -1.8 in β NS cells at site S262. It was also upregulated with a fold change of 2.1 at Y183/M179/M186 in 5 min LPA stimulated β WT cells. These sites identified from MS analysis indicate PI3K activation dependent regulatory sites which can be associated with any kinase along PI3K pathway axis.

Poly(rC) Binding Protein 1 (Pcbp1) has been frequently associated with tumorigenesis and metastasis due to its nucleic acid binding ability. Alongside its iron chaperone activity, it

can mediate interactions with various proteins which take part in messenger RNA processing and transcription through Pcbp1's binding ability to RNA and DNA [39]. In our MS results, functions of transcriptional regulation, RNA binding and metabolism were emphasized in β mutants and stimulated β WT cells. Therefore, Pcbp1 might be connected to p110β induced downstream transcriptional and metabolic activities along PI3K pathway.

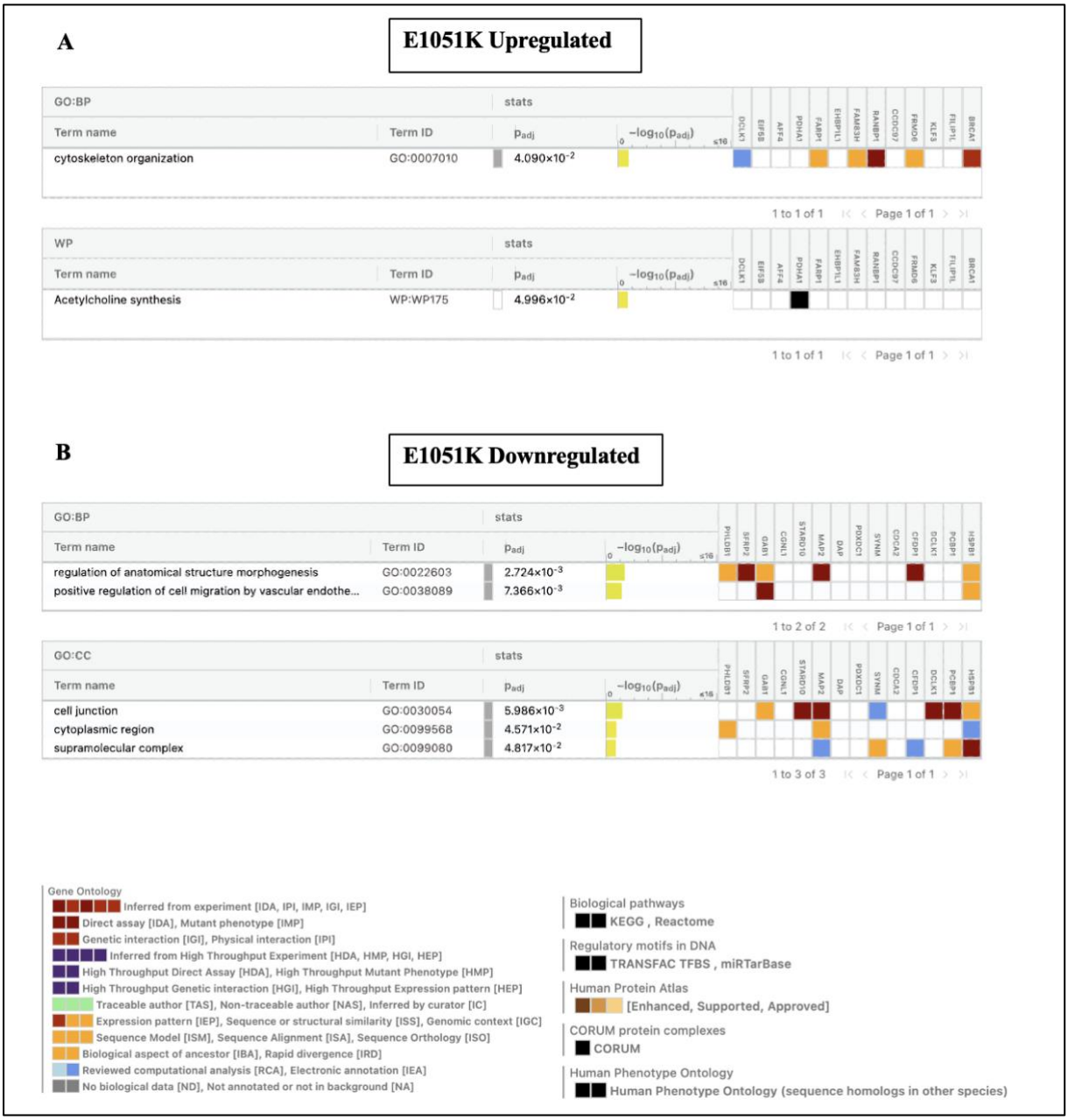

Figure 3.17: Functional enrichment analysis of phosphoproteins up/down-regulated in β EK cells. g:Profiler analysis was conducted for **A)** upregulated **B)** downregulated phosphoproteins found in MS analysis of β EK cells.

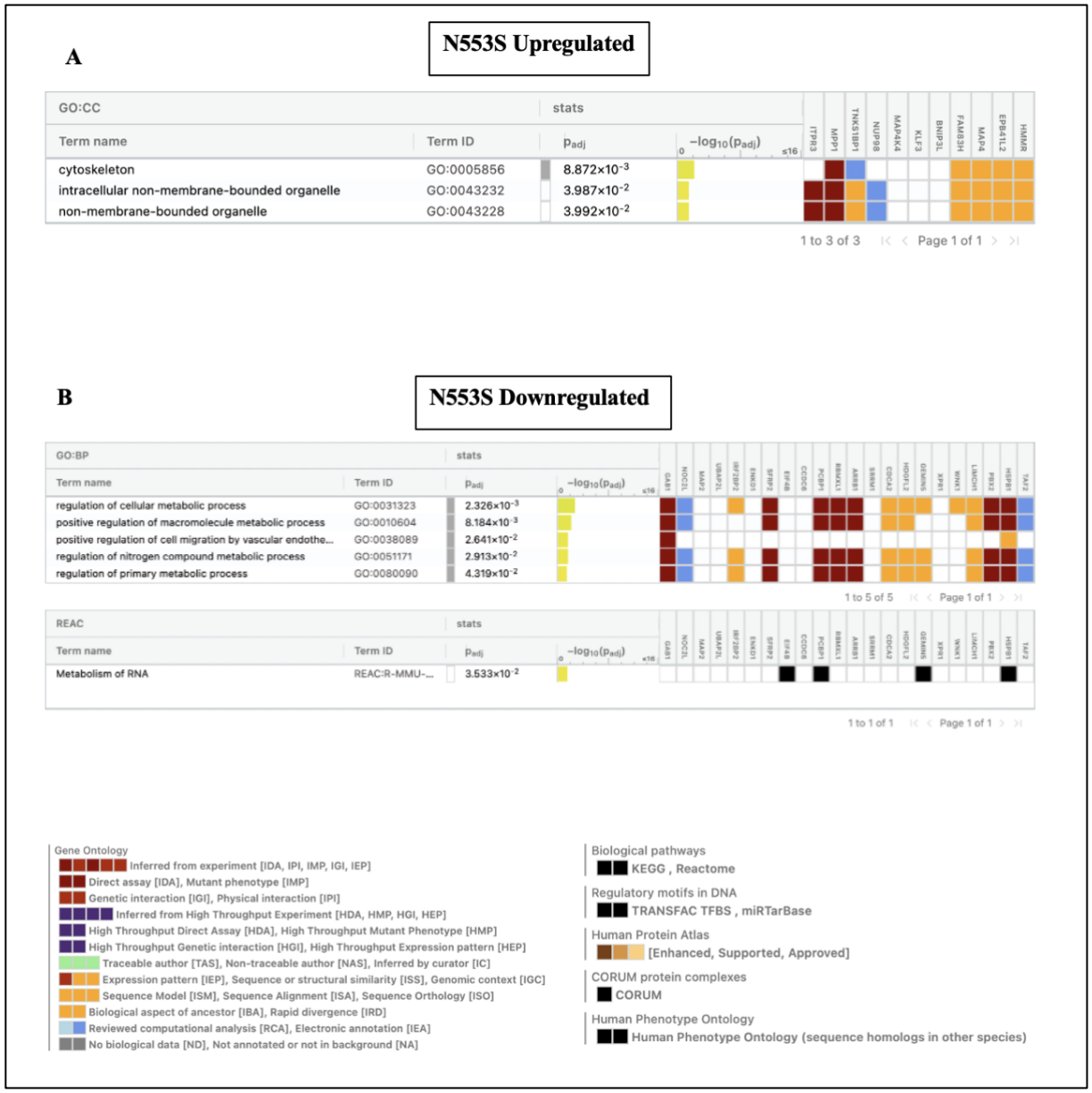

Figure 3.18: Functional enrichment analysis of phosphoproteins up/down-regulated in β NS cells. g:Profiler analysis was conducted for **A)** upregulated **B)** downregulated phosphoproteins found in MS analysis of β EK cells.

4. DISCUSSION

PI3K pathway is one of the critical elements in cancer research due to its frequent activation in various cancer types, especially in prostate and breast cancer. It is one of the primary pathways affecting proliferation and metabolism, and it is commonly associated with the hallmarks of cancer such as survival and metastasis. It also takes part in the construction of the tumour microenvironment through angiogenesis and recruitment of the inflammatory factors.

Class IA PI3Ks are the most commonly studied kinases and they include three different catalytic isoforms: p110α, p110β and p110δ which are encoded by *PIK3CA, PIK3CB* and *PIK3CD* genes. The preliminary data points out PIK3CA amplification and mutations as common hotspots in cancers, however research on PIK3CB and PIK3CD is still in its infancy. Understanding the differences between the functions of these isoforms may pave the way into isoform-specific cancer therapies that might decrease the occurrence of systemic side effects of anti-cancer drugs. This approach might also suggest alternative treatment options to targeted inhibitor treatments which are frequently accompanied by drug-resistance.

This study focuses on the characterization of p110β dependence in Mouse Embryonic Fibroblast (MEF) cells. Based on the data from Cancer Genome Atlas (TCGA) and Memorial Sloan Kettering (MSK) Cancer Center, PIK3CB gene alterations were identified in prostate adenocarcinoma, breast cancer invasive carcinoma and metastatic colorectal cancer. On TCGA database, samples from Cell Journal (2015) have displayed high PIK3CB mRNA levels with gene amplification as the most significant PIK3CB alterations in breast cancer invasive carcinoma, although missense mutations were also identified in some samples [40]. p110β kinase domain mutation E1051K was observed as a hotspot mutation. Overall, PIK3CB alterations resulted in decreased probability of patient survival. Prostate adenocarcinoma was also accompanied with PIK3CB amplifications and missense mutations. MSK data has shown

hotspot E1051K missense mutation as amplified in copy number. Regulatory subunit p85-binding helical domain mutation N553S was also identified in prostate adenocarcinoma samples from Clinical Cancer Research (2022) on MSK database. This data is significant as N553S was only recently identified and no further research has been applied on it. Therefore, our high throughput analysis on N553S mutant brings forth a novel data in cancer research.

Before discussing the mutant analysis, cellular events which take place upon PI3K pathway stimulation must be addressed to understand the downstream protein modifications and interactions caused by p110β dependence. To that end, starvation-stimulation experiments on p110β-dependent β WT cells were conducted with mitogenic stimuli prioritizing either p110β (LPA) or p110α isoform (insulin) along with those that stimulate both isoforms (serum & PDGF) (**Figure 3.1**). The stimulations were performed in two different durations: 5-minute and 30-minute to observe the differences between early and late response events. Although PI3K pathway stimulation has been studied widely before, the time-based approach is novel and it can bring a new perspective into PI3K targeting for cancer therapy.

PI3K pathway activation upon mitogenic stimulation was observed as an increase in Akt phosphorylation. Immunoblotting results have shown that phospho-Akt S473 levels were increased upon stimulation. There was 2-fold difference between serum & PDGF stimulation and p110α specific insulin stimulation. This proves that β WT cells depend on p110β activity primarily for PI3K pathway activation although some residual p110α activity remained which might be due to incomplete deletion of endogenous PIK3CA. Still, these results prove that β WT cells can be considered as a model for p110β-dependent PI3K pathway activation. Moreover, the time dependent approach has shown that PI3K pathway activity increases upon longer periods of stimulation as a 2-fold increase was observed in the levels of pAkt S473 and pS6 S235/236. The downstream substrate analysis by immunoblotting has shown multiple Akt

and PKC substrates in the range of 30-270 kDa (**Figure 3.2**). A distinct band between 30-37 kDa was observed with the same trend as pAkt levels in 5-min stimulations. It should also be noted that the immunoblots of p-Serine and p-Threonine have displayed a time-dependent pattern with increased band intensities at 30-min stimulations. p-Tyrosine bands on the other hand were aligned with p110β-dependent pAkt levels. This might suggest that p110β-dependent downstream phosphorylations on PI3K pathway can be regulated by tyrosine phosphorylations primarily (**Figure 3.3**).

The MS data included multiple Akt and mTOR substrates which were considered as positive controls for this analysis (**Figure 3.4**). Although some phosphorylation sites differed from the canonical Akt and mTOR motifs, it was concluded that these proteins were phosphorylated at non-canonical sites. It must also be noted that proteins obtained from the analysis of p110β-dependent cells were almost completely different than those obtained from p110α-dependent cells, except few which were labelled on **Figure 3.4**.

The early response upregulated phosphoproteins were found to be involved in cellular signaling, transcriptional regulation and RNA binding along with few which were associated with cell motility and cytoskeletal rearrangement. The structural proteins were enhanced among the early response downregulated group and some metabolic proteins were also observed (**Figure 3.5**). The late response upregulated group was enriched with functions of phosphatase activity and cell cycle along with nucleocytoplasmic transport. Ribosomal protein S6 (rpS6) was among them matching with the immunoblotting results. The downregulated late response proteins on the other hand were much fewer in number when compared to the other groups and they showed a disposition for cellular metabolism, dominated by RNA metabolism (**Figure 3.6**). Overall, it can be said that late response activities on PI3K pathway is mainly regulated

by upregulations and more proteins with diverse functions are involved in early response activities.

To compare these results to the PIK3CB mutants, E1051K and N553S MEF cell lines were created. After transduction of MEF cells with dox-inducible PIK3CB E1051K (β EK) and N553S (β NS) vectors, some changes in cell morphologies were observed. β EK cells were smaller in size when compared to the WT line and the common spindle shape of MEF cells transformed into a rounder shape (**Figure 3.7**). These observations were supported with the MS results as various proteins involved in anatomical structure morphogenesis were downregulated in β EK cells (**Figure 3.17**).

Although β EK cells were smaller in size, they duplicated very frequently. β NS cells also proliferated faster than β WT cells (**Figure 3.8 & Figure 3.10**). These proliferative differences were represented as cell viability percentages obtained from SRB proliferation assay results (**Figure 3.9** & **Figure 3.11**). According to these percentages, EK cells displayed resistance to KIN193, a selective p110β inhibitor, treatment. However, both mutants were sensitive to Akt inhibitor MK2206, mTORC1 inhibitor RAD001 (Everolimus) and Rac1 inhibitor EHT1864. Akt and mTORC1 inhibitions were the most effective on the mutants. These results conclude that the proliferative advantage of E1051K and N553S mutants are dependent on Akt and mTORC1 activity. However, E1051K can bypass the inhibitory effects of KIN193 which suggests that either p110β E1051K (β EK) activity is independent of the mechanism by which KIN193 inhibits p110β or this highly tumorigenic mutant can compensate for the inhibitory effects of KIN193.

KIN193 has been used mainly for the treatment of p110β-dependent PTEN-null tumours. It was observed that if p110α does not harbour a gain-of-function mutation, PTEN-loss can

drive p110β-dependence through the upstream GPCR signalling which is the main activator of p110β catalytic isoform. KIN-193 treatment of such tumours resulted in blocked signalling and tumour growth enhanced by PTEN loss [41]. A study on the mechanism of this anti-tumour effect has shown a connection with apoptotic regulators in Bcl-2 family proteins. Bcl-2 consists of three subfamilies including pro-apoptotic and anti-apoptotic molecules [42]. Bcl-2 and Bcl-X_L belong to one subfamily and they inhibit apoptosis induced by reactive oxygen species (ROS) after localization to smooth endoplasmic reticulum and mitochondria. On the other hand, Bax which is a member of another subfamily is a dimer that promotes apoptosis by changing the mitochondrial outer membrane permeability upon receival of apoptotic signals.

A study on the effect of KIN193 on nasopharyngeal carcinoma (NPC) proved that the number of Bcl2 positive cells in NPC tumours were reduced upon KIN193 treatment and tumour cell death was enhanced. However, Bax levels were upregulated. These results suggested that the ratio of Bcl2 and Bax plays an important role in cell survival and apoptosis. By upregulating Bax and downregulating Bcl2 in the cell, KIN193 can mediate mitochondrial outer membrane permeability. Moreover, Caspase 9, an initiator of apoptosis and activator of Caspase 3, was observed in its active cleaved state after KIN193 treatment. Therefore, it was concluded that Caspase 9 along with Bcl2 and Bax play an important function in the mechanism of KIN193 anti-tumour activity [43]. This mechanism could also be related to the resistance to KIN193 in β EK cells. Although neither of these proteins were found in MS results, their regulation and activity might be altered in EK mutants. It should also be noted that Bcl2 Associated Transcription Factor 1 (Bclaf1) was found among the upregulated late response group, phosphorylated at S267 with a fold change of 2.8. It functions as a transcriptional repressor and interacts with Bcl2 family members [44]. Bcl2 interacting protein 3 like (Bnip3l) which is a member of pro-apoptotic subfamily of Bcl2 protein family [45]. It was upregulated in β NS cells at S61 with a fold change of 1.7.

β EK and NS cells were also investigated for the differences between their effectors downstream of PI3K pathway. Similar to β WT cells, Akt and PKC substrate immunoblots of the mutants displayed various bands between 30-270 kDa. Despite the similarity between β WT and mutants, the banding pattern for MEF WT cells were quite different. This result emphasizes the tumorigenic effects of p110β amplification (**Figure 3.13**). Interestingly, the band observed between 30-37 kDa on the immunoblots of β WT stimulation samples was also seen on the substrate blots of β EK and β NS. Since RpS6 is a common Akt substrate at 32 kDa, by co-immunoprecipitating RpS6 with Akt substrates it was investigated if 30-37 kDa band observed on substrate blots belonged to RpS6. It was concluded that the band corresponds to another Akt substrate (**Figure 3.15**).

The analysis of the phosphoproteomic MS data of β EK & NS cells have shown proteins distinct for each mutant. They also varied from the phosphoproteins compiled for p110α-dependent cells and its catalytic (H1047R) and helical (E545K) domain mutants. Few proteins common for both isoforms were indicated (**Figure 3.16**). Akt and mTOR substrates were again identified as positive controls of this MS analysis.

The upregulated β EK phosphoproteins were mostly related to cytoskeletal organization and cellular migration. As expected, some tumour suppressors and oncogene proteins were also identified in the upregulated phosphoproteome of this highly tumorigenic catalytic subunit mutant. Interestingly, proteins involved in the regulation of cellular anatomical structure were among the downregulated phosphoproteins. This result aligned with the morphological changes observed for β EK cells under microscope (**Figure 3.7**). Some proteins involved in cellular metabolism were also observed.

Most of the upregulated β NS phosphoproteins were involved in structural organization and microtubule assembly. Few proteins also associated with nuclear import and apoptotic regulation. The downregulated phosphoproteins on the other hand were mostly related to cellular metabolism; RNA metabolism proteins were especially abundant. Functions of cellular signalling and transcriptional regulation were also highlighted. Proteins involved in various mechanisms of transcriptional regulation were found.

An Akt substrate Poly(rC) Binding Protein 1 (Pcbp1) was identified as a 37 kDa protein downregulated at S262 in both β EK & NS cells. It was also upregulated in 5-min LPA stimulated β WT cells at Y183. These findings align with the pAkt substrates results obtained by immunoblotting (**Figure 3.2 & Figure 3.13**). Although the latest research on Pcbp1 is focused on its recently found iron chaperone activity, Pcbp1 has long been studied in the context of tumour progression and metastasis. Due to its nucleic acid binding property, Pcbp1 has an important role in coordinating RNA molecules and thus gene expression. It was first identified as a constituent of heterogeneous nuclear ribonucleoprotein (hnRNPs) complexes. It has an impact on transcription, messenger RNA processing, stability, and translation [46]. It was downregulated in various cancers and its upregulation was linked to reduced metastasis and epithelial-to-mesenchymal transition (EMT). Therefore, it was suggested as a tumor suppressor [47].

The PCBP1 gene locus has been described as a tumour suppressor gene region and it was found that this region also gives rise to a long noncoding RNA (lncRNA), PCBP1-AS1 which is encoded from 462 bp upstream of PCBP1 coding sequence [46]. A negative correlation between the expression levels of PCBP1 and PCBP1-AS1 was observed [48]. Research on the roles of lncRNAs on hepatocellular carcinoma (HCC) metastasis has shown that PCBP1-AS1 levels were increased in HCC tissues and the levels correlated with reduced patient survival and

increased metastasis. It was also observed that PCBP1-AS1 silencing affected the expression of PCBP1 and its downstream genes PRL-3 and p-AKT. A significant increase was observed in the levels of both PRL-3 and p-Akt S473 & T308 upon the overexpression of PCBP1-AS1 while the levels decreased after the its knockdown. It was concluded that PCBP1-AS1 induces HCC tumour progression and metastasis through binding PCBP1 and regulating PCBP1-PRL3-AKT signalling axis [48].

Phosphatase of regenerating liver-3 (PRL-3) has also been associated with metastasis and its overexpression resulted in increased invasiveness and cell motility, indicators of EMT. Upon overexpression of PRL-3 in human colorectal cancer cell line DLD-1, cells were treated with a pan-PI3K inhibitor LY294002. After PI3K inhibition, it was shown that the effects of PRL-3 on epithelial and mesenchymal markers were blocked. PTEN levels were also decreased in DLD-1 cells upon the overexpression of PRL-3.

In the same study, it was shown in PRL-3 overexpressing HeLa cells that cell motility was increased through reduced levels of paxillin (Pxn) and phospho-paxillin (Y31), focal adhesion protein vinculin and other focal adhesion complexes [49]. Y31 and Y118 phosphorylations of Pxn have been reported as essential for the proper localization and function of Pxn in the cell [50]. Pxn is among the main components of focal adhesions and as a scaffolding protein it recruits various kinases, phosphatases and structural proteins involved in cellular signalling. Activation of these pathways result in actin cytoskeleton reorganization and assembly or disassembly of focal adhesions. Therefore, it was reported that Pxn can either promote or impede cell migration [51]. In our MS data, Pxn was found downregulated at Y118 with fold changes of -1.6 and -1.7 in 5-min serum and LPA stimulation groups respectively. Although it requires more research, tyrosine-phosphorylated Pxn downstream signalling was associated with the activity of Rho family GTPases. This hypothesis can also connect our findings to

p110β-dependent oncogenesis in the cell which is mainly induced by GPCR and small G-protein activity.

As a tumour suppressor affecting PI3K signalling through PRL3 activity, Pcbp1 can be considered as a candidate protein to study the mechanisms of oncogenesis in the case of p110β dependence. Due to its RNA-binding activity, Pcbp1 implements various mechanism of transcriptional regulation on cancer-related genes. It has been associated with the inhibition of tumour progression through mRNA stability regulation in ovarian cancer. Pcbp1 mutations have been frequently observed in colon cancer. Downregulation of Pcbp1 was followed by increased tumour stemness and metastasis in prostate and breast cancer. Peritoneal metastasis was also observed upon downregulation of Pcbp1 in pancreatic and gastric cancer [52]. The MS analysis of stimulated β WT cells, and β EK & NS mutants also revealed phosphoproteomic regulations on proteins involved in transcriptional regulation, mRNA binding, processing and metabolism, along with apoptotic regulation, tumorigenesis, cytoskeletal reorganization and cell migration. Together with the previous findings, these results indicate a critical role for p110β in tumour progression.

5. CONCLUSION & FUTURE PERSPECTIVES

Although p110α isoform of PI3K and its mutants has been widely studied and associated with cancer, the significance of p110β isoform has not been brought to light yet. Previous studies have shown that unlike its Class IA isoform which is dominantly activated by RTK signalling, p110β relies mostly on GPCR and small G-protein activity. Also, p110β dependence has been frequently observed in tumours with PTEN-loss. In this study, we conducted a high throughput downstream phosphoproteomic analysis on p110β-dependent WT or p110β mutant MEF cells. Dox-inducible PIK3CB WT (β WT) and PIK3CB E1051K (β EK) & N553S (β NS)

mutant MEF cell lines were created with retroviral transduction and the endogenous PIK3CB and PIK3CA were deleted with Cre Recombinase systems. Some morphological differences in β EK cells have shown some morphological differences post-transduction; cells became smaller in size and fewer spindles were identified at the cell edges when compared to the WT MEF cell morphology. The cell viability also increased in β EK & NS cells. SRB proliferation assay results have shown that β EK cells are resistant to p110β-specific inhibition by KIN193, the mechanism of which is dependent on the regulation of apoptotic protein levels in the cell. On the other hand, Akt and mTORC1 inhibitions decreased cell viability dramatically in both mutants.

Various mitogenic stimulants were applied on β WT cells for two different durations. Changes in PI3K downstream protein levels were checked with immunoblotting. p110α-specific insulin stimulation was less effective on PI3K downstream phosphorylations when compared to p110β-specific LPA and other mitogens stimulating both isoforms. Moreover, late response proteins caused an amplification on the PI3K downstream activation. A distinct 30-37 kDa band on the downstream substrate analysis was observed and it was regulated in a p110β-dependent manner. The same band was also seen on the downstream substrate blots of β EK & NS mutants. The immunoblots of the mutants have shown upregulated PI3K downstream phosphorylations when compared to MEF WT and β WT cells.

These results were supported by LC-MS/MS analysis. Phosphoproteomic MS results for stimulated β WT cells have shown different regulations for various proteins when compared to the starvation group. Early response proteins were mostly associated with transcriptional regulation, cytoskeletal rearrangement, cellular signalling, migration and metabolism when late response proteins were involved in cell cycle progression, phosphatase activity, nucleocytoplasmic transport and RNA metabolism. In LPA stimulated cells, 37 kDa Akt

substrate Poly(rC) Binding Protein 1 (Pcbp1) was observed as an early response upregulated protein at site Y183.

Similar to stimulated early response proteins in β WT cells, the phosphoproteome of β EK cells were also associated with cytoskeletal rearrangement and cellular migration. Aligning with the previous morphological observations, proteins involved in anatomical structure regulation were observed. Some tumour suppressors and oncogene proteins were also among the differentially regulated phosphoproteins. On the other hand, the phosphoproteome of β NS cells were enriched for functions of RNA metabolism, nuclear import and apoptotic regulation similar to the late response proteins, along with others involved in structural organization and microtubule assembly. Interestingly, Pcbp1 was again found among the phosphoproteome of both β EK & NS cells, downregulated at S262.

We have suggested Pcbp1 as a candidate protein to study p110β-dependence as it is a critical RNA-binding protein (RBP) coordinating the stability and processing of various RNA molecules and therefore gene expression. The changes in its cellular levels were observed to affect metastasis and EMT in the previous studies. Since our results have shown that p110β isoform has a major role in cytoskeletal reorganization, cell migration and transcriptional regulation, studying the regulation of p110β-Pcbp1 axis can pave the way to understand the mechanisms of disposition for increased tumour progression in p110β-dependent cells. To that end, the cellular levels of Pcbp1 along with EMT markers can be investigated in stimulated and mutant cells. Since RNA coordination with RBPs is essential for the nucleocytoplasmic transport and RNA processing, the link between p110β activity and Pcbp1 function can be assessed by studying the cellular localization of proteins involved in cellular migration and metastasis in the presence and absence of functional Pcbp1. Cytoskeletal proteins such as Paxillin and focal adhesion proteins can also be investigated in terms of expression with

immunoblotting and cellular distribution by immunofluorescence. These experiments can also be conducted in different cell types such as epithelial or cancer cells instead of fibroblasts.

6. BIBLIOGRAPHY

[1] O. Cizmecioglu, J. Ni, S. Xie, J. J. Zhao, and T. M. Roberts, "Rac1-mediated membrane raft localization of PI3K/p110β is required for its activation by GPCRs or PTEN loss," *Elife*, vol. 5, Oct. 2016, doi: 10.7554/eLife.17635.

[2] BioRender, "PI3K Pathway in Cancer," *BioRender.com*, 2022. https://app.biorender.com/illustrations/63a9a5242b1f3780064c2ca2 (accessed Dec. 26, 2022).

[3] J. Yang, J. Nie, X. Ma, Y. Wei, Y. Peng, and X. Wei, "Targeting PI3K in cancer: mechanisms and advances in clinical trials," *Mol Cancer*, vol. 18, no. 1, p. 26, Dec. 2019, doi: 10.1186/s12943-019-0954-x.

[4] M. Graupera *et al.*, "Angiogenesis selectively requires the p110α isoform of PI3K to control endothelial cell migration," *Nature*, vol. 453, no. 7195, pp. 662–666, May 2008, doi: 10.1038/nature06892.

[5] R. Fritsch *et al.*, "RAS and RHO Families of GTPases Directly Regulate Distinct Phosphoinositide 3-Kinase Isoforms," *Cell*, vol. 153, no. 5, pp. 1050–1063, May 2013, doi: 10.1016/j.cell.2013.04.031.

[6] T. Utermark *et al.*, "The p110α and p110β isoforms of PI3K play divergent roles in mammary gland development and tumorigenesis," *Genes Dev*, vol. 26, no. 14, pp. 1573–1586, Jul. 2012, doi: 10.1101/gad.191973.112.

[7] S. Jia *et al.*, "Essential roles of PI(3)K–p110β in cell growth, metabolism and tumorigenesis," *Nature*, vol. 454, no. 7205, pp. 776–779, Aug. 2008, doi: 10.1038/nature07091.

[8] J. Qu *et al.*, “PIK3CB is involved in metastasis through the regulation of cell adhesion to collagen I in pancreatic cancer,” *J Adv Res*, vol. 33, pp. 127–140, Nov. 2021, doi: 10.1016/j.jare.2021.02.002.

[9] M. Shodell and H. Rubin, “Studies on the Nature of Serum Stimulation of Proliferation in Cell Culture,” *In Vitro*, vol. 6, no. 1, pp. 66–74, 1970.

[10] H. Zhang *et al.*, “PDGFRs are critical for PI3K/Akt activation and negatively regulated by mTOR,” *Journal of Clinical Investigation*, vol. 117, no. 3, pp. 730–738, Mar. 2007, doi: 10.1172/JCI28984.

[11] Ma. E. Díaz *et al.*, “Growth hormone modulation of EGF-induced PI3K-Akt pathway in mice liver,” *Cell Signal*, vol. 24, no. 2, pp. 514–523, Feb. 2012, doi: 10.1016/j.cellsig.2011.10.001.

[12] J. J. Zhao *et al.*, “The p110α isoform of PI3K is essential for proper growth factor signaling and oncogenic transformation,” *Proceedings of the National Academy of Sciences*, vol. 103, no. 44, pp. 16296–16300, Oct. 2006, doi: 10.1073/pnas.0607899103.

[13] B. D. Hopkins, M. D. Goncalves, and L. C. Cantley, “Insulin–PI3K signalling: an evolutionarily insulated metabolic driver of cancer,” *Nat Rev Endocrinol*, vol. 16, no. 5, pp. 276–283, May 2020, doi: 10.1038/s41574-020-0329-9.

[14] M. E. Li *et al.*, “Role of p110a subunit of PI3-kinase in skeletal muscle mitochondrial homeostasis and metabolism,” *Nat Commun*, vol. 10, no. 1, p. 3412, Jul. 2019, doi: 10.1038/s41467-019-11265-y.

[15] V. R. Sopasakis *et al.*, “Specific Roles of the p110α Isoform of Phosphatidylinsositol 3-Kinase in Hepatic Insulin Signaling and Metabolic Regulation,” *Cell Metab*, vol. 11, no. 3, pp. 220–230, Mar. 2010, doi: 10.1016/j.cmet.2010.02.002.

[16] A. Riaz, Y. Huang, and S. Johansson, “G-Protein-Coupled Lysophosphatidic Acid Receptors and Their Regulation of AKT Signaling,” *Int J Mol Sci*, vol. 17, no. 2, p. 215, Feb. 2016, doi: 10.3390/ijms17020215.

[17] Y. Nakanishi *et al.*, “Activating Mutations in *PIK3CB* Confer Resistance to PI3K Inhibition and Define a Novel Oncogenic Role for p110β,” *Cancer Res*, vol. 76, no. 5, pp. 1193–1203, Mar. 2016, doi: 10.1158/0008-5472.CAN-15-2201.

[18] The Jackson Library, “PIK3CA Gene H1047R Variant Detail,” *CKB CORE*, 2016.

[19] The Jackson Library, “PIK3CA Gene E545K Variant Detail,” *CKB CORE*, 2016.

[20] H. Leontiadou, I. Galdadas, C. Athanasiou, and Z. Cournia, “Insights into the mechanism of the PIK3CA E545K activating mutation using MD simulations,” *Sci Rep*, vol. 8, no. 1, p. 15544, Oct. 2018, doi: 10.1038/s41598-018-27044-6.

[21] Vandebilt-Ingram Cancer Center, “PIK3CA Amplification,” *My Cancer Genome*, 2017.

[22] J. Shi *et al.*, “Highly frequent PIK3CA amplification is associated with poor prognosis in gastric cancer,” *BMC Cancer*, vol. 12, no. 1, p. 50, Dec. 2012, doi: 10.1186/1471-2407-12-50.

[23] The UniProt Consortium, “P42336 · PK3CA_HUMAN,” *UniProt*, 2022.

[24] Y. Nakanishi *et al.*, “Activating Mutations in *PIK3CB* Confer Resistance to PI3K Inhibition and Define a Novel Oncogenic Role for p110β,” *Cancer Res*, vol. 76, no. 5, pp. 1193–1203, Mar. 2016, doi: 10.1158/0008-5472.CAN-15-2201.

[25] A. D. Whale, L. Colman, L. Lensun, H. L. Rogers, and S. J. Shuttleworth, “Functional characterization of a novel somatic oncogenic mutation of PIK3CB,” *Signal Transduct Target Ther*, vol. 2, no. 1, p. 17063, Dec. 2017, doi: 10.1038/sigtrans.2017.63.

[26] Vandebilt-Ingram Cancer Center, “PIK3CB D1067Y,” *My Cancer Genome*, 2017.

[27] The UniProt Consortium, “P42338 · PK3CB_HUMAN,” *UniProt*, 2022.

[28] A. J. Takeda *et al.*, "Novel PIK3CD mutations affecting N-terminal residues of p110δ cause activated PI3Kδ syndrome (APDS) in humans," *Journal of Allergy and Clinical Immunology*, vol. 140, no. 4, pp. 1152-1156.e10, Oct. 2017, doi: 10.1016/j.jaci.2017.03.026.

[29] K. Vogan, "PIK3CD mutations cause immunodeficiency," *Nat Genet*, vol. 45, no. 12, pp. 1417–1417, Dec. 2013, doi: 10.1038/ng.2840.

[30] The UniProt Consortium, "O00329 · PK3CD_HUMAN," *UniProt*, 2022.

[31] O. Cizmecioglu, J. Ni, S. Xie, J. J. Zhao, and T. M. Roberts, "Rac1-mediated membrane raft localization of PI3K/p110β is required for its activation by GPCRs or PTEN loss," *Elife*, vol. 5, Oct. 2016, doi: 10.7554/eLife.17635.

[32] L. S. Moniz *et al.*, "Phosphoproteomic comparison of Pik3ca and Pten signalling identifies the nucleotidase NT5C as a novel AKT substrate," *Sci Rep*, vol. 7, Jan. 2017, doi: 10.1038/srep39985.

[33] J. C. Obenauer, L. C. Cantley, and M. B. Yaffe, "Scansite 2.0: Proteome-wide prediction of cell signaling interactions using short sequence motifs," *Nucleic Acids Res*, 2003.

[34] P. V. et al Hornbeck, "PhosphoSitePlus, 2014: mutations, PTMs and recalibrations," *Nucleic Acids Res*, 2015.

[35] W. H. Zheng, S. Kar, and R. Quirion, "Stimulation of protein kinase C modulates insulin-like growth factor-1- induced Akt activation in PC12 cells," *Journal of Biological Chemistry*, vol. 275, no. 18, pp. 13377–13385, May 2000, doi: 10.1074/jbc.275.18.13377.

[36] A. H. Hsu *et al.*, "Crosstalk between PKCα and PI3K/AKT Signaling Is Tumor Suppressive in the Endometrium," *Cell Rep*, vol. 24, no. 3, pp. 655–669, Jul. 2018, doi: 10.1016/j.celrep.2018.06.067.

[37] D. Szklarczyk *et al.*, “The STRING database in 2023: protein–protein association networks and functional enrichment analyses for any sequenced genome of interest,” *Nucleic Acids Res*, vol. 51, no. D1, pp. D638–D646, Jan. 2023, doi: 10.1093/nar/gkac1000.

[38] Uku Raudvere *et al.*, “g:Profiler: a web server for functional enrichment analysis and conversion of gene lists,” *Nucleic Acids Research*, 2019.

[39] S. J. Patel, O. Protchenko, M. Shakoury-Elizeh, E. Baratz, S. Jadhav, and C. C. Philpott, “The iron chaperone and nucleic acid–binding activities of poly(rC)-binding protein 1 are separable and independently essential,” *Proceedings of the National Academy of Sciences*, vol. 118, no. 25, Jun. 2021, doi: 10.1073/pnas.2104666118.

[40] J. Gao *et al.*, “Integrative Analysis of Complex Cancer Genomics and Clinical Profiles Using the cBioPortal,” *Sci Signal*, vol. 6, no. 269, Apr. 2013, doi: 10.1126/scisignal.2004088.

[41] J. Ni *et al.*, “Functional Characterization of an Isoform-Selective Inhibitor of PI3K-p110β as a Potential Anticancer Agent,” *Cancer Discov*, vol. 2, no. 5, pp. 425–433, May 2012, doi: 10.1158/2159-8290.CD-12-0003.

[42] Y. Tsujimoto, “Role of Bcl-2 family proteins in apoptosis: apoptosomes or mitochondria?,” *Genes to Cells*, vol. 3, no. 11, pp. 697–707, Nov. 1998, doi: 10.1046/j.1365-2443.1998.00223.x.

[43] F. Chen, A. Zheng, F. Li, S. Wen, S. Chen, and Z. Tao, “In vivo and in vitro investigation of KIN-193 anti-tumor effects on nasopharyngeal carcinoma,” *Transl Cancer Res*, vol. 9, no. 1, pp. 49–57, Jan. 2020, doi: 10.21037/tcr.2019.11.03.

[44] National Library of Medicine, “BCLAF1 BCL2 associated transcription factor 1 [Homo sapiens (human)],” *NCBI*, Aug. 2023.

[45] National Library of Medicine, “BNIP3L BCL2 interacting protein 3 like [Homo sapiens (human)],” *NCBI*, Jul. 2023.

[46] S. J. Patel, O. Protchenko, M. Shakoury-Elizeh, E. Baratz, S. Jadhav, and C. C. Philpott, “The iron chaperone and nucleic acid–binding activities of poly(rC)-binding protein 1 are separable and independently essential,” *Proceedings of the National Academy of Sciences*, vol. 118, no. 25, Jun. 2021, doi: 10.1073/pnas.2104666118.

[47] S. Huang, K. Luo, L. Jiang, X.-D. Zhang, Y.-H. Lv, and R.-F. Li, “PCBP1 regulates the transcription and alternative splicing of metastasis-related genes and pathways in hepatocellular carcinoma,” *Sci Rep*, vol. 11, no. 1, p. 23356, Dec. 2021, doi: 10.1038/s41598-021-02642-z.

[48] T. Luo *et al.*, “ lncRNA PCBP1-AS1 Aggravates the Progression of Hepatocellular Carcinoma via Regulating PCBP1/PRL-3/AKT Pathway ,” *Cancer Manag Res*, vol. Volume 12, pp. 5395–5408, Jul. 2020, doi: 10.2147/CMAR.S249657.

[49] H. Wang, S. Y. Quah, J. M. Dong, E. Manser, J. P. Tang, and Q. Zeng, “PRL-3 Down-regulates PTEN Expression and Signals through PI3K to Promote Epithelial-Mesenchymal Transition,” *Cancer Res*, vol. 67, no. 7, pp. 2922–2926, Apr. 2007, doi: 10.1158/0008-5472.CAN-06-3598.

[50] K. Nakamura, H. Yano, H. Uchida, S. Hashimoto, E. Schaefer, and H. Sabe, “Tyrosine phosphorylation of paxillin α is involved in temporospatial regulation of paxillin-containing focal adhesion formation and F-actin organization in motile cells,” *Journal of Biological Chemistry*, vol. 275, no. 35, pp. 27155–27164, Sep. 2000, doi: 10.1074/jbc.M000679200.

[51] A. M. López-Colomé, I. Lee-Rivera, R. Benavides-Hidalgo, and E. López, “Paxillin: a crossroad in pathological cell migration,” *J Hematol Oncol*, vol. 10, no. 1, p. 50, Dec. 2017, doi: 10.1186/s13045-017-0418-y.

[52] Y. Zheng *et al.*, “The RNA-binding protein PCBP1 represses lung adenocarcinoma progression by stabilizing DKK1 mRNA and subsequently downregulating β-catenin,” *J Transl Med*, vol. 20, no. 1, p. 343, Dec. 2022, doi: 10.1186/s12967-022-03552-y.